

# Naposomes: a new class of peptide-derivatized, target-selective multimodal nanoparticles for imaging and therapeutic applications

Modified supramolecular aggregates for selective delivery of contrast agents and/or drugs are examined with a focus on a new class of peptide-derivatized nanoparticles: naposomes. These nanoparticles are based on the co-aggregation of two different amphiphilic monomers that give aggregates of different shapes and sizes (micelles, vesicles and liposomes) with diameters ranging between 10 and 300 nm. Structural properties and *in vitro* and *in vivo* behaviors are discussed. For the high relaxitivity values (12–19 $mM^{-1}s^{-1}$) and to detect for the presence of a surface-exposed peptide, the new peptide-derived supramolecular aggregates are very promising candidates as target-selective MRI contrast agents. The efficiency of surface-exposed peptides in homing these nanovectors to a specific target introduces promising new opportunities for the development of diagnostic and therapeutic agents with high specificity toward the biological target and reduced toxic side effects on nontarget organs.

## Supramolecular aggregates as carriers of active principles

Supramolecular aggregates such as micelles and liposomes, obtained by aggregation of amphiphilic compounds **(Figure 1)**, have attracted great attention for their potential application as *in vivo* carriers of active principles. In the early 1970s, the use of liposomes as drug-carrier systems was proposed by Gregoriadis & Ryman [1]. They are considered nontoxic, biodegradable and non-immunogenic. Owing to their size, which typically ranges in mean diameter from 50 to 300 nm for the systemically administered compounds, liposomes display some unique pharmacokinetic characteristics. These include clearance via the reticuloendothelial system (RES), which results in a relatively long systemic circulation time, and hepatic and splenic distribution. Furthermore, liposomes exhibit preferential extravasation and accumulation at the site of solid tumors due to increased endothelial permeability and reduced lymphatic drainage in these tissues, which has been defined as the enhanced permeability and retention effect [2]. On the other hand, the composition of the molecules used for the formation of the vesicular structure will, at least, affect the fate of liposomes from the site of their introduction as well as their interaction with components of the body (e.g., surface charge [3–6], serum proteins, lipoproteins, the opsonin system [7,8], the phagocytic system [9] and finally target cells [8,10,11]). The hydrophobic core of micelles and the inner cavity of liposomes are carrier compartments that accommodate a large amount of drugs or contrast agents, while the shell, consisting of brush-like protecting corona, stabilizes the drugs in aqueous solution and reduces toxicity of the active principle in nontarget organs. Associating a drug with liposomes markedly changes its pharmacokinetic and pharmacodynamic properties and lowers systemic toxicity; furthermore, the drug is prevented from early degradation and/or inactivation after introduction to the target organism [12–17]. In systemic administration of reporter compounds, micelles or liposomes should respect several base requirements: high loading capacity of a drug and/or contrast agent, biodegradability, long blood circulation times, slow plasma clearance and controllable drug-release profiles.

Examples of drugs in liposomal formulations are reported in **Table 1**. The most active drugs against breast cancer are currently the anthracyclines and taxanes (paclitaxel and docetaxel). Many research efforts have been directed towards improving the safety profile of the anthracycline cytotoxics, doxorubicin (DOX) and daunorubicin (DNR), along with vincristine, which are associated with severe cardiotoxic side effects, although acute gastrointestinal effects and other

**Antonella Accardo[1], Anna Morisco[1], Diego Tesauro[1], Carlo Pedone[1] & Giancarlo Morelli[†1]**

Department of Biological Sciences & CIRPeB – University of Naples 'Federico II', Via Mezzocannone 16, 80134 Naples, Italy
[†]Author for correspondence:
Tel.: +39 081 253 6650
E-mail: gmorelli@unina.it

FUTURE SCIENCE part of fsg

**Key Term**

**Delivery systems:** A single bioactive molecule or a supramolecular aggregate such as a micelle or a liposome able to carry a drug or a contrast agent for *in vivo* applications.

toxicities may also occur. For example, the alkylating agent DOX acts by intercalating into DNA and has been used in the liposomal formulation known as Doxil®. This liposomal DOX formulation showed increased time in circulation and decreased cardiovascular-related toxicity when compared with free DOX [18]; whereas, encapsulated DOX liposomes combined with cyclophosphamide, in an experimental pulmonary metastatic melanoma mouse model, showed high anti-tumor effect [19].

Strategies for the delivery of taxanes are under active investigation to increase tumor exposure and/or to reduce adverse effects such as neurotoxicity, edema, asthenia and alopecia. In addition, special issues with the taxanes provide further rationale for the application of **delivery systems**. Both paclitaxel and docetaxel are poorly soluble in aqueous solutions, and have consequently been formulated with Cremaphor EL and polysorbate 80 (TWEEN 80), respectively. Unfortunately, these formulations are highly allergenic, require extensive premedication, and are responsible for most of the acute toxicities observed with taxane therapy, rather than the taxanes themselves. Consequently, alternative delivery strategies based on liposome-encapsulated paclitaxel [20] and poly(L-glutamic acid)-paclitaxel, a polymer conjugate [21], have been developed and tested in clinical trials.

Other liposomal drugs in breast cancer include approved chemotherapic drugs such as vinca alkaloids, platinums and camptothecins. Moreover, development of alternative classes of potent anticancer agents based on liposome-based systems for delivery of nucleic acids, such as antisense oligonucleotides and gene therapy constructs are currently under investigation.

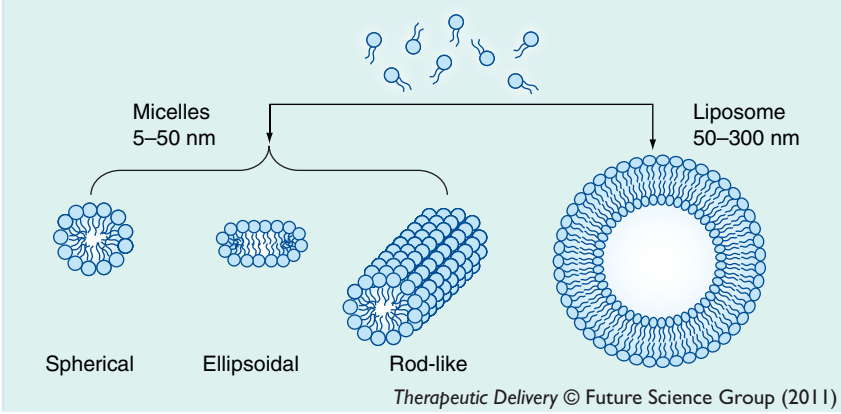


**Figure 1. Supramolecular aggregates (micelles and liposomes) obtained by assembling amphiphilic molecules consisting of a hydrophobic and a hydrophilic moiety in aqueous solution.**

A liposomal formulation of amphotericin B and AmBisome, is a potent antifungal drug currently used for the treatment of invasive aspergillosis. Upon administration, AmBisome remains intact in the blood and distributes to the tissues where fungal infections may occur [11]. Disruption of AmBisome is observed after attachment to the outside of fungal cells, resulting in fungal cell death. Although AmBisome exhibits less *in vitro* antifungal activity than amphotericin B in some cases [11,22–24], much higher doses of AmBisome can be administered safely, resulting in an improved therapeutic profile [25].

Moreover, Mayer *et al.* have investigated the application of liposomes as a delivery vehicle for drug combinations [26]. The use of drug combinations is a widely adopted strategy in clinical cancer therapy. Combinations of irinotecan/fluoxuridine, DNR/cytarabine, cisplatin/DNR and DOX/verapamil was shown to be highly effective against cells that are multidrug resistant [27].

Several supramolecular aggregates have also been developed as carriers of contrast agents in MRI. They are based on multimeric or macromolecular contrast agents in which a large number of paramagnetic gadolinium (Gd) complexes are combined together and the total relaxivity, that is the critical parameter to have contrast in MRI images, results from the single contribution of each Gd ion [28,29]. In particular, three classes of nonspecific contrast agents have been developed:

- Aggregates obtained directly by the self-assembly of amphiphilic chelating agents;
- Mixed aggregates containing synthetic amphiphilic chelating agents and one or more commercial phospholipids;
- Self-assembling aggregates of polymeric amphiphiles that incorporate contrast agents.

Micelles and liposomes are taken up to a large extent by the RES. This property makes supramolecular aggregates excellent candidates as possible carriers of Gd(III)-chelates to enhance the contrast efficacy and to change the pharmacokinetic properties of MRI contrast agents. The first studies on the use of liposomes as carriers of MRI contrast agents appeared in the literature in the 1980s [30–32]. There have been two main approaches in the development of liposomal contrast agents: in the first one, contrast agents are entrapped within the internal

**Table 1. Examples of drugs in liposomal formulations.**

| Drug | Application | Commercial name | Composition of liposomes |
|---|---|---|---|
| Amikacin | Bacterial infections | MiKasome™ | HSPC/CH/DSPG |
| Adriamycin (DOX) | Stomach cancer | – | DPPC/CH |
| Ampicilin | Listeria monocytogenes | – | CH:PC:PS (5:4:1)<br>CH:DSPC:DPPG (10:10:1) |
| Annamycin | Kaposi's sarcoma<br>breast cancer, leukemia | Annamycin | DMPC:DMPG (7:3) |
| Amphotericin B[11,22–25] | Systemic fungal infections | AmBisome® | HSPC/CH/DSPG |
| All–*trans*-retinoic acid | Acute promyelocytic leukemia, lymphoma, prostate cancer | ATRAGEN® | DMPC/soybean oil |
| Muramyl dipeptide | Immunostimulator | – | DSPC:PS (1:1) |
| 1-β-D-arabinofuranozidecytozine | Leukemia | – | SM/PC:CH (1:1:1) |
| Ciprofloxacine | *Pseudomonas aeruginosa* | – | DPPC |
| Clodronate | Macrophage suppression | – | PC/CH |
| *Cis*-diaminodichloro-platinum(II) | Cancers | – | PS/PC |
| Cyclosporin | Immunosuppressor | – | PC/CH |
| Chloroquine | Malaria | – | PC:PG:CH (10:1:5) |
| Cu/Zn superoxide dismutase | Anti-inflammatory | – | DPPC:CH:stearylamine (7:2:1) |
| DOX [18] | Cancers | Myocet® | PC:CH (5:5) |
| DOX [19] | Cancers | Doxil | HSPC/CH/PEG–DSPE |
| DOX | Breast cancer | EVACET™ | eggPC:chol (55:45) |
| Daunorubicin | Cancers | DaunoXome® | DSPC/CH |
| Ganciclovir | Cytomegalovirus retinitis | – | PC/CH:sodium deoxycholate (12:1.7:1) |
| IL-2 | Immunostimulant | – | DMPC |
| Leukotriene A4 | Not estimated | – | PC:DCP:CH (7:2:1) |
| Lipid A | Immunoadjuvant | – | DMPC:DMPG/CH (0.9:0.1:0.75) |
| Mitoxantron | Colon cancer | – | PC:CH (7:1) |
| Methotrexate | Cancers | – | DPPC:PI (18:2 w/w) |
| Nystatin | Systemic fungal infections | NYOTRAN™ | DMPC: DMPG (7:3) |
| Na3(B20H17NH3) | Cancers | – | DSPC/CH |
| Platinum drugs (e.g., cisplatin) | Mezotelioma | PLATAR | *bis*-NDDP |
| Lurtotecan | Cancers | NX 211 | HSPC:CH (2:1) |
| Oligonucleotides against *c–myc* | Cancers | INXC–6295 | DSPC/CH/DODAP/PEGCerC14 (25:45:20:10) |
| Prostaglandin E1 | Anti-inflammatory | – | PC |
| Ribavirin | Herpes simplex | – | DPPC:CH:DCP (2.0:1.5:0.22) |
| Streptosotocin | Lymphocyte activator | – | DMPC:CH (2:1) |
| Suramin | Trypanosomes | – | DPPC |
| Muramyl tripeptide | Immunostimulant | – | PC:PS (7:3) |
| Vincristin | Cancers | VincaXome | DSPC/CH |
| Vincristin | Cancers, lymphoma | Onco TCS | DSPC/CH |
| Various drugs and contrasts | Diagnostics of various diseases | LipoMASC™ | PEG–liposomes |

*CH: Cholesterol; DCP: Dicetylphosphate; DMPC: Dimyristoylphosphatidylcholine; DMPG: Dimyristoyl phosphatidylglycerol; DODAP: 1,2-dioleoyl-3-dimethyl-ammonium propane; DPPC: Dipalmitoylphosphatidylcholine; DPPG: Dipalmitoylphosphatidylglycerol; DSPC: Distearoylphosphatidylcholine; DSPG: Distearoylphosphatidylglycerol; DOX: Doxorubicin; HSPC: Hydrogenated soya phosphatidylcholine (hydrogenated soya lecithin); NDDP: Neodecanoate diaminocyclohexane platinum; PC: Phosphatidylcholine; PegCerC14: 1-O-(2'-(w-methoxy-polyethyleneglycol) succinoyl)-2-N-myristoylsphingosine; PEG–DSPE: Polyethylene glycol-phosphatidylethanolamine derivative; PEG-liposomes: Liposomes modified with components containing a polyethylene glycol; PG: Phosphatidylglycerol; PI: Phosphatidylinositol; PS: Phosphatidylserine; SM: Sphingomyelin.*

aqueous space of liposomes [30]; in the second approach, lipophilic contrast agents are incorporated in the lipid bilayer of the liposom [31,32]. Classical Gd complexes such as Gd–diethylenetriamine penta-acetic acid (DTPA), Gd–DTPA-*bis*(methoxyethylamide), and Gd–HPDO3A have been loaded within the internal aqueous space of lipid vesicles: the main target for such supramolecular aggregates is the liver, given the avid accumulation of these aggregates by Kupffer cells, and the relatively slow clearance of the Gd complexes once internalized [33]. While

studying blood concentrations of these aggregates to evaluate the possibility of using these liposomes for MRI application, it was observed that the enhancement of relaxivity is limited, as it is approximately two- to five-times lower compared with the same concentrations of free Gd complexes in solution. The relaxivity of the entrapped paramagnetic species appears to be lowered because of the limited exchange of bulk water with the contrast agents [30,34] under these conditions. This slow exchange is caused by the low permeability of the liposomal membrane to water [35]. Thus the second approach, where a hydrophilic chelating agent is covalently linked to a hydrophobic chain, may be more effective. In this scheme, the lipid part of the molecule is anchored in the liposome bilayer while the more hydrophilic Gd complex is localized on the liposome surface [36,37]. Several chelating probes of this type have been developed for liposome membrane incorporation. This approach results in an improved ionic relaxivity of the metal compared with the approach of encapsulating the paramagnetic molecules in the aqueous interior liposomal space, and compared with low molecular weight (MW) complexes [38]. None of the studied liposomal aggregates derivatized with paramagnetic Gd complexes have reached the market.

## Target-selective supramolecular aggregates

Labeling of supramolecular aggregates with bioactive markers able to direct them toward specific biological target receptors has led to next generation delivery systems for active principles [39]. The bioactive markers commonly used to prepare target-selective supramolecular aggregates are peptides and antibodies [40–42]. Entire antibodies, or their fragments also present the advantage of maintaining their *in vivo* stability and binding properties when coupled to supramolecular aggregates. However, their high MW could prevent bioavailability and circulation properties of the full aggregate; on the contrary low MW peptides, if they remain stable *in vivo*, well exposed on the aggregate surface, and in appropriate conformation for binding to a target receptor, could be more promising tools for selective delivery of supramolecular aggregates to the cellular target.

Different synthetic procedures have been developed to introduce bioactive molecules to the external surface of the supramolecular aggregate [43]. The choice of synthetic strategy depends on whether coupling is performed before or after assembly of the supramolecular aggregate. The obvious goal of each approach is to achieve high coupling efficiency, but with the ligand retaining full binding affinity for its target receptor. The coupling of a ligand after the aggregate has been assembled involves the introduction of suitable activated functional groups onto the terminus of one of the aggregate components. Activated functional groups must be compatible with the aggregation process and should remain available on the aggregate surface for efficient chemical ligation of the bioactive ligand. As schematized in **Figure 2**, route 1, an example of this approach consists in the preparation of liposomes or micelles containing a 1,2-distearoyl-sn-glycero-3-phosphoethanolamine-*N*-(maleimide) (DSPE)-polyethylene glycol (PEG) monomer derivatized with a *N*-maleimido function on the distal end of the DSPE–PEG monomer; after aggregate formation the externally exposed *N*-maleimido function reacts with the bioactive molecule, according to the sulphydryl–maleimide coupling method, to give the labeled supramolecular aggregate. Another example of this approach is based on the obtainment of biotinylated aggregates using a biotinylated liphophilic monomer in the surfactant mixture; in a two-step process the biotinylated supramolecular aggregates react with avidin and then with the biotinylated peptide or antibody giving a noncovalently labeled compound (**Figure 2**, route 2). This strategy has proven to be particularly successful for the coupling of large ligands such as monoclonal antibodies. The coupling of a bioactive ligand to an aggregate component before aggregation is, in principle, chemically less complicated, but has the disadvantage that, at least in the case of liposomes, following final assembly of the aggregate a fraction of the conjugated bioactive ligand remains entrapped in the interior region and is not more available for receptor binding. This labeling procedure, based on the use of amphiphilic peptides that assemble together with other amphiphilic monomers in the peptide-labeled supramolecular aggregates, is schematized in **Figure 2**, route 3.

These procedures have been successfully developed to prepare target-selective supramolecular aggregates, labeled with bioactive markers and loaded with active drugs acting as target-selective drug carriers [42,44], or, if labeled with a pool of Gd complexes, acting as target-selective MRI contrast agents [45–47].

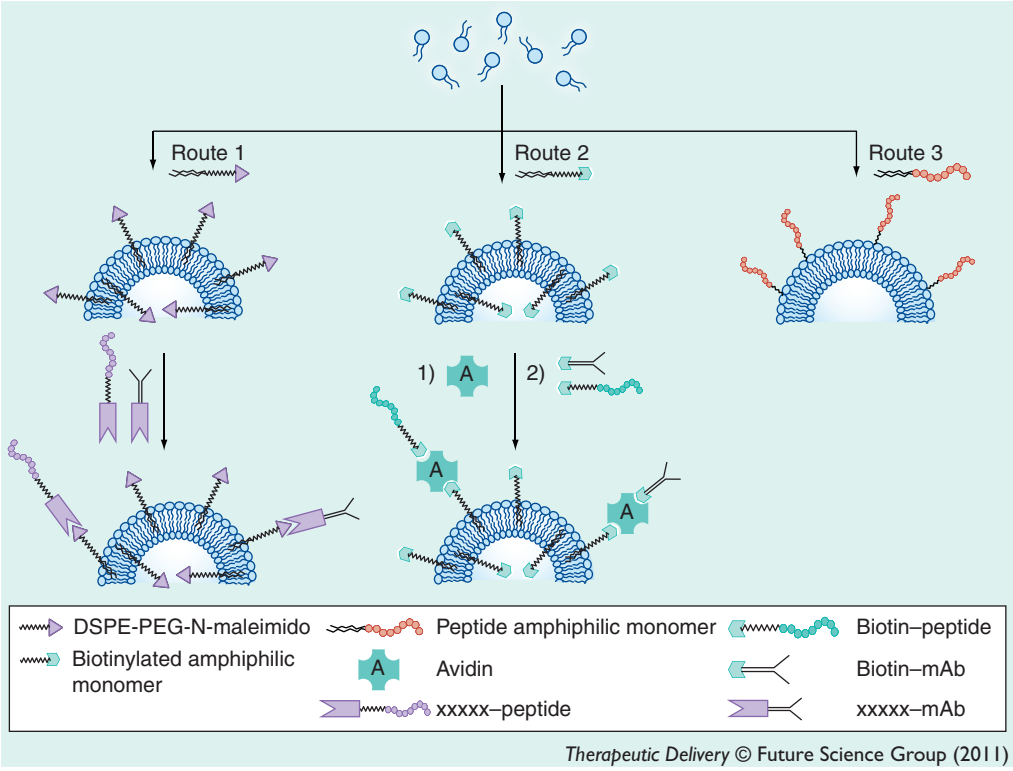


*Therapeutic Delivery* © Future Science Group (2011)

**Figure 2. Three routes for liposome labeling by bioactive molecules.** According to **route 1**, a polyethylene glycol-phosphatidylethanolamine derivative monomer derivatized with a *N*-maleimido function is incorporated in the liposomes; after aggregate formation the externally exposed *N*-maleimido function reacts with the bioactive molecule to give the labeled supramolecular aggregate. In another approach **(route 2)**, biotinylated aggregates are obtained by using a biotin-bearing lipophilic tail in the surfactant mixture; successively, in a two-step process, the biotinylated supramolecular aggregates react with the protein avidin, then biotinylated peptides or antibodies interact in free avidin sites giving a noncovalently labeled compound. In the last case **(route 3)**, labeled aggregates are obtained by co-assembling amphiphilic peptides and other surfactants. DSPE-PEG-*N*-maleimido: Polyethylene glycol-phosphatidylethanolamine derivative monomer derivatized with a *N*-maleimido.

For example, PEGylated paramagnetic liposomes (immuno-liposomes) derivatized with antibody molecules that are coupled to the distal end of PEG chains have been developed [48]. The chosen antibody is able to detect E-selectin expression on human umbilical vein endothelial cells, this is an attractive model for receptor expression on endothelial cells. The same authors described the use of PEGylated, fluorescent and paramagnetic micelles (immuno-micelles) for imaging of macrophages in atherosclerotic plaques [49]. Another approach followed was anchoring the antibody to a biotin–avidin complex [50–54]. This system allows the labeling of mixed micelles previously formulated combining the amphiphilic Gd complex, the phospholipids and the TWEEN 80 surfactant. The *ex vivo* images [50] and *in vivo* experiments confirmed that this kind of immuno-micelles provides excellent validated *in vivo* enhancement of atherosclerotic plaques [51].

The same approach was used formulating polymerized vesicles by UV irradiation of a mixture of Gd-DTPA polymerizable lipid, a polymerizable biotinilated lipid and diacetylene phosphatidilcholine filler lipid [52–54], followed by derivatization of the liposomes with LM609 monoclonal antibody capable of *in vivo* detection of tumor angiogenesis targeting the integrin $\alpha_v\beta_3$ [54]. Similar antibody-conjugated paramagnetic polymerized liposomes were used to target the intercellular adhesion molecule-1, an endothelial leukocyte receptor on cerebral microvasculature in experimental autoimmune encephalitis [55].

Gadolinium-based paramagnetic supramolecular aggregates derivatized with bioactive peptides have essentially been developed in order to have selective contrast agents capable of visualizing neovascularization and angiogenic processes targeting $\alpha_v\beta_3$ integrins or tumor proliferation

**Key Term**

**Multimodal nanoparticles:** Nanoparticles derivatized with a drug and a contrast agent for different applications, and with bioactive or protective compounds to improve their *in vivo* biodistribution and stability.

and metastasis targeting cellular receptors that are overexpressed by cancer cells. Some interesting supramolecular constructs were initially developed by Stupp and co-workers by self-assembly of amphiphile RGD (Arg-Gly-Asp) peptide sequences carrying a 1,4,7,10-tetraazacyclododecane-1,4,7,10-tetraacetic acid (DOTA)–Gd(III) complex [47,56]. These amphiphilic molecules self-assemble into spherical and fiber-like nanostructures [47]. Liposomes, conjugated with the $\alpha_v\beta_3$-specific RGD peptide attached to PEG moieties, have been developed by Mulder and co-workers [57,58]. *In vitro* studies demonstrate that RGD-liposomes associate impressively with proliferating endothelial cells associated with cancer, they are internalized by the cells and localized to a perinuclear compartment. *In vivo* studies indicate that RGD-liposomes are localized at the rim of the tumor with a distribution pattern that closely correlates with the position of angiogenic blood vessels in the tumor, which are found mainly at the rim. Moreover, these nanoparticles can be used, by MRI techniques, to non-invasively measure the efficacy of angiogenesis inhibitors during the course of a therapy [58].

Griffioen and co-workers used Anginex, a synthetic 33-mer angiostatic peptide that is capable of homing to activated endothelium, as targeting ligand [59]. Paramagnetic liposomes obtained by co-aggregation of Gd–DTPA lipid and maleimide–PEG2000–DSPE, derivatized with Anginex was studied *in vitro* on cell cultures and by MRI of cell pellets. The results indicate that Anginex is a potent ligand for the targeting of activated endothelial cells; in addition, the *in vitro* results showed a high specificity of the anginex-conjugated paramagnetic liposomes for endothelial cells that was confirmed by MRI.

## Naposomes: a new class of peptide-derivatized target-selective multimodal nanoparticles

Multimodal supramolecular compounds that combine together imaging and therapeutic capabilities are the focus of intensive research for applications in the growing field of nanomedicine. They offer the prospective to increase diagnostic accuracy and therapeutic effectiveness, while minimizing side effects from treatment [60,61].

In recent years we developed a new class of peptide-derivatized target-selective **multimodal nanoparticles** for imaging and therapeutic applications identified as 'naposomes'.

Naposomes, with their micellar or liposomal structure can encapsulate active pharmaceutical principles and are promising candidates for such multifunctional therapeutic platforms since they are functionalized on their external surface with a reporter peptide to achieve specific and selective delivery to target cells and contain chelating agents able to give stable metal complexes for diagnostic applications such as imaging by MRI or positron emission tomography (PET) and scintigraphy.

These materials are conveniently synthesized, and can be assembled to a range of sizes and compositions [62]. They are obtained by co-assembling two amphiphilic monomers: a first monomer containing a hydrophobic moiety, a spacer and a bioactive peptide having high affinity for membrane receptors expressed by target cells, and a second monomer based on the same hydrophobic moiety of the first monomer and containing a chelating agent able to complex several metal ions with high stability. **Figure 3** shows the two amphiphilic monomers and supramolecular aggregates that can be obtained when monomers are combined at the chosen molecular ratio in water solution. Several parameters such as pH, ionic strength, monomer composition and formulation procedure (dissolution in buffered solution or well-assessed procedures based on sonication and extrusion) can influence the size and shape of the aggregates, which includes: spherical or ellipsoidal micelles, cylindrical or elongated micelles, open bilayers or liposomes. All these supramolecular aggregates are characterized by the presence of the bioactive peptide well exposed on the external surface of the aggregate, while the chelating agents, or their metal complexes, remain on the aggregate hydrophilic shell. Only in the case of liposomes are peptides and chelating agents equally divided between the external aggregate surface and the inner aqueous compartment.

The hydrophobic moieties present on both monomers are based on one or two hydrocarbon chains, saturated hydrocarbon chains with 18 carbon atoms are the most widely hydrophobic moieties used in naposome preparation. The spacer introduced, in the first monomer, between the bioactive peptide and the hydrophobic moiety is very important to allow the peptide to remain well exposed on the external surface of the aggregate and to maintain its high binding affinity, in the nanomolar range, to the membrane receptors expressed by target cells. Oxoethylene and polyethylene linkers of different MW have been tentatively used to define the best length to preserve peptide exposition and bioavailability.

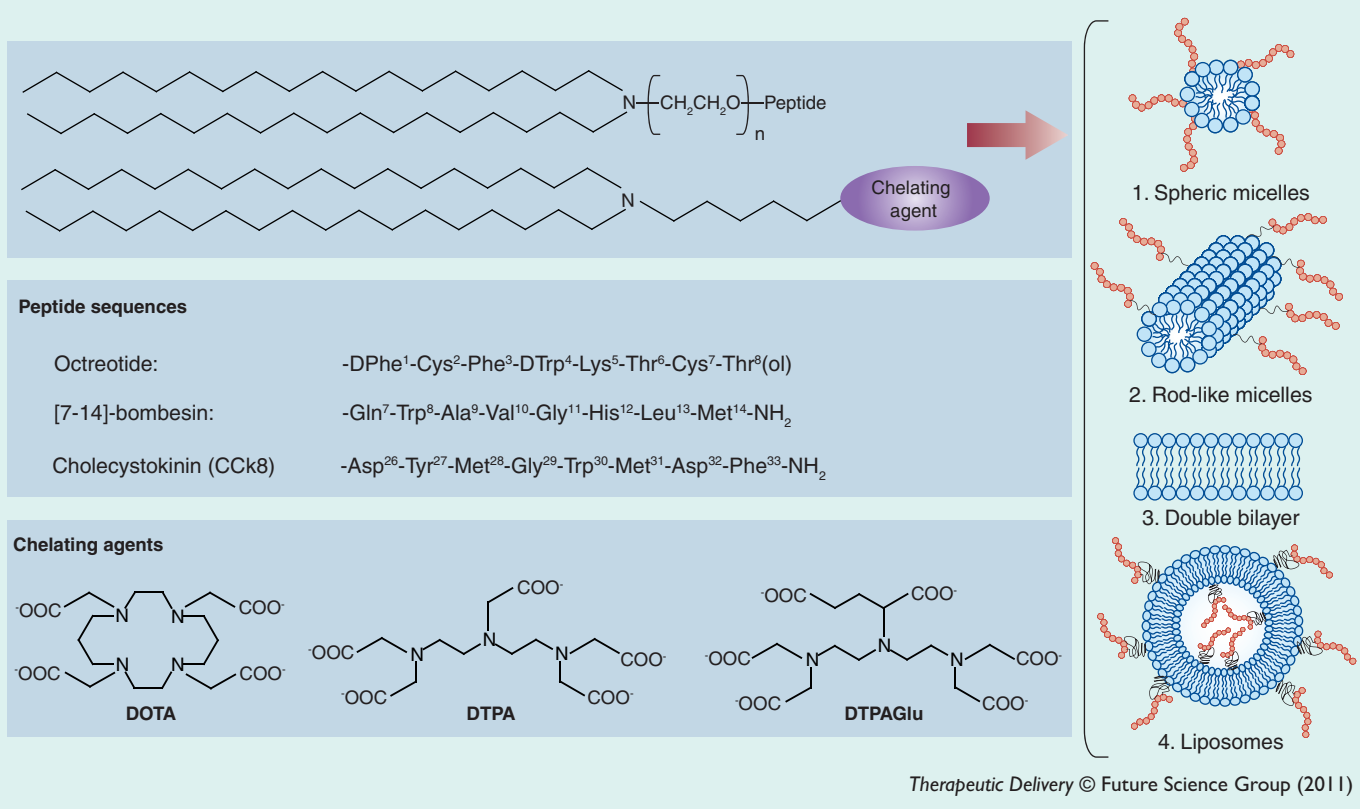


**Figure 3. Representation of two monomers: one containing a peptide moiety and the other containing the chelating agent.** By combining the two monomers, mixed aggregates with different size and shape are obtained, as indicated on the right of the figure. In the two frameworks, the peptide sequences (octrotide, 7-14-bombesin and CCK8) and the structure of chelating agents used for naposomes preparation are reported.

The spacer in the second monomer is usually a lysine residue. It is introduced between the hydrophobic moiety and the chelating agent, for synthetic reasons. In fact, the lysine residue, with its three active functions, can be linked through the carboxy function to a solid support allowing solid-phase synthesis of the entire monomer by selective reactions of the α and ε amino groups with the hydrophobic moiety and the chelating agent, respectively.

The chelating agents used in naposome preparation are branched or cyclic polyamino-polycarboxy ligands: DTPA and its glutamic analog DTPAGlu are branched ligands with five or six carboxylic functions, respectively; DOTA is a cyclic chelating agent with four carboxylic functions and four amino groups. In all chelating agents, one carboxylic function is used to link the chelating agent to a lysine side chain in the amphiphilic monomer, while the other carboxylic functions and the amino groups form the coordinative set for several metal ions, thus giving thermodynamically stable and kinetic inert metal complexes. Metal complexes of Gd(III) for MRI applications, of $^{111}$In(III) for scintigraphic imaging and of Ga(III) for PET tomography, have been obtained.

Until now, naposomes have been prepared by using three different peptides: CCK8 [63–74], 7-14-bombesin (BN) [75] and octreotide [76,77]. These peptides are well known endogenous (CCK8 and BN) or artificial (octreotide) ligands for membrane receptors overexpressed by cells of several human cancers.

CCK8 corresponds to the eight-residue C-terminal end of the cholecystokinin peptide hormone [78], and has been widely studied for its high binding affinity, in the nanomolar range, towards the two cholecystokinin receptors, CCK1-R and CCK2-R [79]. These receptors represent very important targets for selective therapeutic delivery being found overexpressed in pancreatic cancers, meningiomas and neuroblastomas (CCK1-R) and in small-cell lung cancer, colon and gastric cancers, medullar thyroid carcinomas and stromal ovarian tumors (CCK2-R) [80,81]. Moreover, the NMR solution structures of the complexes between CCK8 and

receptor fragments have also been reported; analysis of the structure indicates that modification on the N-terminus of CCK8 does not interfere with the binding region [82]. This hypothesis has been widely confirmed by the behavior of CCK8 derivatives containing bulky substituents on the N-terminus: CCK8-modified compounds that contain radioactive metal ions complexed by branched or cyclic chelating agents introduced on the peptide N-terminus, present receptor-binding properties in the same nanomolar range of the unmodified CCK8 peptide and have been proposed as target-selective contrast agents for nuclear medicine techniques [83].

7-14-bombesin is the C-terminal fragment of BN peptide and it binds members of the BN receptor family that consists of four receptor subtypes including the neuromedin B receptor, the gastrin-releasing peptide receptor, the orphan receptor subtype, and the amphibian receptor [84–87]. The expression of gastrin-releasing peptide receptors is found in several human cancer cell lines, such as prostate, breast cancer, small-cell lung cancer and ovarian cancer [88–90]. Also 7-14-BN derivatives modified on the N-terminus with radioactive metal complexes are used as target-selective contrast agents for scintigraphic and PET images, while peptide derivatives containing β-emitting radionuclides on the N-terminus have been proposed as target-selective radiotherapeutics [91]. octreotide is a well known synthetic cyclic peptide widely used as an *in vivo* stable somatostatin analog [92]. It binds the somatostatin receptors (SSTRs), in particular the SSTR2 and SSTR5 receptor sub-types [93,94] and is pharmacologically used as a somatostatin analog in many therapeutic procedures that need somatostatin, such as pituitary adenomas. octreotide derivatives labeled with $^{111}$In complexed by DTPA linked to peptide N-terminus (Octroscan®) are clinically used as scintigraphic contrast agents [95] to evidence the overexpression of SSTRs in several human tumors such as neuroendocrin tumors, tumors of the nervous system, lymphomas and some breast cancers [96–99].

The membrane receptor overexpression in several clinically relevant human tumors together with the finding that these peptides can be modified on their N-terminal end without substantial loss of their receptor-binding affinity, suggested the use of these three peptides in naposome development.

Other endogenous peptides able to target membrane receptors overexpressed in pathological conditions could be explored to develop new target-selective nanoparticles for delivery of therapeutic and/or contrast agents. Neurotensin, vasointestinal peptide, neuropeptide Y, their stable fragments or their peptide analogs acting as agonist or antagonists seem the best candidates to develop other peptide-modified supramolecular aggregates [100].

Four different classes of naposomes have been developed to date. They are based on the use of different amphiphilic monomers, as schematized in **Figure 4**. In any case, amphiphilic monomers are synthesized by using solid-phase procedures. The peptide-containing monomer is synthesized starting from the C-terminal end: the last amino acid in the peptide sequence is bound to the resin acting as solid support, then 9-fluorenylmethyloxycarbonyl (Fmoc) deprotection and coupling steps are performed according to classic procedures for peptide synthesis in solid phase and using the Fmoc/*tert*-butyl chemistry. After the peptide synthesis is complete, and analytically certified, one or more oxoethylene spacers or PEG derivatives are linked to the peptide N-terminus, using Fmoc–amino–oxoethylene- or Fmoc–amino–PEG-protected derivatives containing a carboxylic function that is activated *in situ* by using classic coupling reagents. After Fmoc deprotection the hydrophobic moiety is bound by using an aliphatic

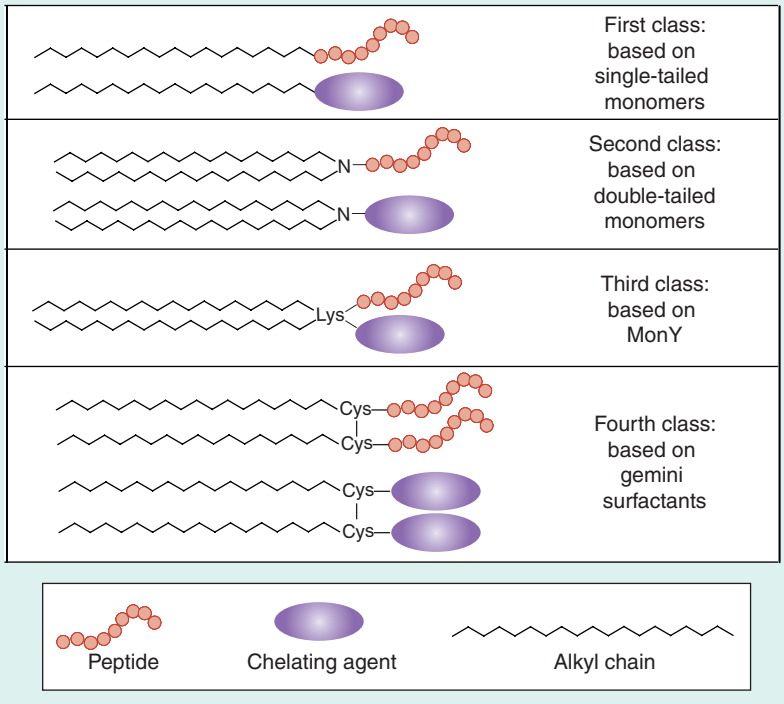


**Figure 4. Four classes of naposomes.**

amine linked to a succinic spacer. At the end of the solid-phase synthesis the monomer is cleaved from the resin and purified by HPLC. In addition, the second monomer is prepared by using solid-phase methods: a lysine residue, containing orthogonal protecting groups on the two amino functions, is linked through the carboxylic function to the resin, then the α and ε lysine amino groups selectively react with the hydrophobic moiety and the chelating agent, respectively. Chelating agents containing all the carboxylic acid functions, except that used to bound the ε lysine amino function (which is protected as a *tert*-butyl ester) are used.

The two monomers are combined in mixed supramolecular aggregates in buffered water solution, simply mixing them in solution or by using classical procedures to prepare liposomes based on the preparation of a lipid film in organic solvent, the film dissolution in buffered water solution followed by sonication and extrusion procedures. The two monomers are combined together using a defined molecular ratio, usually the chelating agent-containing monomer is the more abundant monomer and the peptide-containing monomer is present in a lower amount, between 3 and 30% of the total. In some cases other phospholipids are also added in the final composition.

### ■ First-class naposomes

The first class of naposomes is based on two amphiphilic monomers containing a single-tailed hydrophobic monomer with 18 carbon atoms, the CCK8 peptide, in the first monomer, as a target-selective tool, and DTPAGlu as chelating agent, able to complex paramagnetic Gd ions, in the second monomer [63,64]. They have been prepared in order to obtain mixed micelles to be used as new potential target-selective contrast agents in MRI. This was the first attempt to form a supramolecular aggregate containing a bioactive molecule able to deliver a large amount of paramagnetic Gd ions to a specific place, that is, where tumor cells are present.

The two monomers C18DTPAGlu(Gd) and C18L×CCK8 (× = 2, 5) are schematized in the framework of **FIGURE 5**. Two different peptide monomers have been synthesized, one in which the linker between the alkyl chain and the peptide is composed by two oxoethylene moieties and a glycine residue ($C18L_2CCK8$), and the other with a larger number (five) of oxoethylene linkers ($C18L_5CCK8$). The mixed aggregates (**FIGURE 5**, right side), obtained by combining the two monomers in a molar ratio between 95:5 and 70:30, as well as the pure C18DTPAGlu aggregate, in the presence and absence of Gd(III), have been fully characterized by surface tension measurements, FT-PGSE-NMR, fluorescence quenching, fluorescence spectroscopy, and small-angle neutron scattering (SANS) measurements. In all cases the two monomers, C18DTPAGlu (or C18DTPAGlu([Gd]) and $C18L_2CCK8$, form mixed spherical micelles (critical micelle concentration [cmc] ~$5 \times 10^{-5}$ mol $kg^{-1}$) with an external shell of approximately 21 Å, an inner core of approximately 20 Å and an aggregation number, $N_{agg}$, of approximately 65. Both the DTPAGlu(Gd) complexes and the CCK8 peptides point toward the external micelle surface. Formation of mixed aggregates is confirmed by self-diffusion experiments and SANS measurements. In fact, the NMR signals of the two monomers never showed a multi-exponential decay, indicating that the two monomers co-micellize and, consequently, diffuse together. Moreover, the magnitude of the SANS scattering profile of the C18DTPAGlu–C18LxCCK8 system with respect to the pure C18DTPAGlu system showed a significant increase in intensity, suggesting the formation of mixed micelles **(FIGURE 5A)**. Mixed micelles based on $C18L_5CCK8$ showed similar properties with respect to micelles based on $C18L_2CCK8$, although the hydrodynamic radius was found to be a slightly larger 37 Å. This behavior is due to the $C18L_5CCK8$ insertion in the mixed aggregates that promotes the formation of more elongated micelles. The SANS data in this case show a reasonably good fit, also using an ellipsoid model. Moreover, the structural data analysis suggests that the bioactive CCK8 peptide is not completely exposed on the external micelle surface in systems containing $C18L_2CCK8$. The length of the oxoethylene linkers and glycine residues could be too short to allow an efficient exposure of CCK8 at the surface. According to crystallographic data of PEG, a chain of two oxoethylene linkers has a linear dimension of approximately 12 Å; whereas, the thickness of the hydrophilic DTPAGlu shell of the mixed micelle is approximately 18 Å. Hence, a considerable part of the bioactive peptide in $C18L_2CCK8$ is probably hidden among the DTPAGlu moieties, reducing the chance that the aggregates could bind to the membrane proteins overexpressed by tumor cells. In contrast, in the case of mixed micelles containing $C18L_5CCK8$ there is a complete exposure of the CCK8 peptide externally to the micelles. The length of

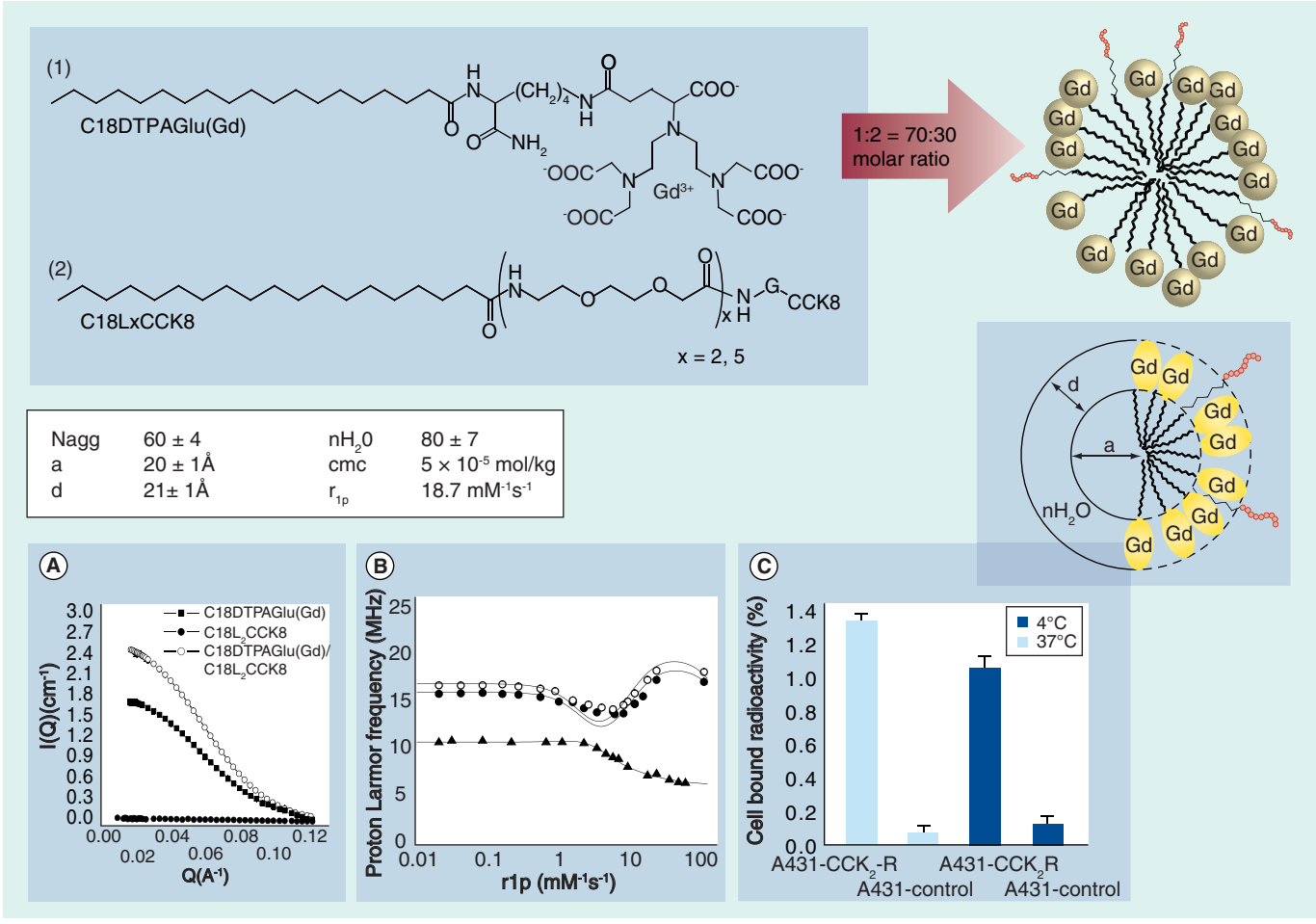


**Figure 5. First class of naposomes, based on single-tailed monomers.** Schematic representation of C18DTPAGlu(Gd) and C18LxCCK8 (x = 2, 5) monomers. Right-hand side of figure: schematic representation of micelles obtained by mixing together the two monomers in a 70:30 molar ratio is reported. In the table, structural data and relaxometric properties are summarized. Bottom of figure: **(A)** scattering intensity profile for C18DTPAGlu(Gd) and $C18L_2CCK8$ binary systems and C18DTPAGlu(Gd)/$C18L_2CCK8$ ternary system; **(B)** NMR dispersion profiles of C18DTPAGlu(Gd)/$C18L_2CCK8$ (○), C18DTPAGlu(Gd) (•) and DTPAGlu(Gd) complex (▲) at pH 7.4 and 298 K, normalized to 1 mM concentration of Gd(III) ion; **(C)** binding assays of radio-labeled mixed aggregates C18DTPAGlu/$C18L_5CCK8$ on A431 cells overexpressing CCK2-R at 4 and 37°C.

the spacer (five oxoethylenes) is approximately 30 Å, a value quite a bit larger than the shell thickness. Substantial structural differences were not found when the C18DTPAGlu or its Gd complex C18DTPAGlu(Gd) were used for aggregate preparation even if the C18DTPAGlu monomer contains five negative charges on the chelating agent, while the Gd monomer complex remains with only two negative charges. The measured values for relaxivity, in a saline medium at 20 MHz proton Larmor Frequency and 25°C, for Gd complexes in the pure C18DTPAGlu(Gd) micelles and for the mixed systems are 17.5 and 18.7 $mM^{-1}s^{-1}$, respectively **(Figure 5B)**. These values are in good agreement with those reported in the literature for supramolecular aggregates obtained by self-assembling mono-tailed amphiphilic monomers and indicate a large enhancement in comparison with that of isolated DTPAGlu(Gd) complex in water solution (6.2 $mM^{-1}s^{-1}$).

Receptor-binding ability of micelles belonging to the first class of naposomes was evaluated by standard nuclear medicine experiments **(Figure 5C)**. Micelles obtained by co-assembling C18DTPAGlu/$C18L_5CCK8$ in a 70:30 molar ratio, are labeled with the γ-emitting radionuclide $^{111}In$. This metal ion is complexed by DTPAGlu chelating agent by incubation of preformed micelles, at aggregate concentrations above the cmc to avoid presence of free monomers in solution, with $InCl_3$ at room temperature. According to classical labeling procedures used in nuclear medicine techniques, only a small

percentage of the DTPAGlu chelating agents are present on the hydrophilic monomer complexes; despite this, in radionuclides the total amount is enough to study the binding properties of the entire aggregate. Binding experiments are performed on A431 (a human epidermoid carcinoma cell line) cultured cells overexpressing the $CCK_2$-R by stable transfection and compared with control cells. Since a certain degree of nonspecific binding and internalization of the aggregates was expected, experiments are performed both at 4°C (in order to block cellular metabolic processes such as nonspecific internalization) and at 37°C (to keep metabolic processes active). Similar results are obtained under the two experimental conditions indicating receptor targeting specificity and negligible nonspecific binding and internalization **(FIGURE 5C)**.

It is worth noting that, in general, micelles respond rapidly to changes in their environment, while bilayers are much more sluggish. These results are of crucial importance for the use of this class of target selective contrast agents from the clinical point of view. In fact, in order to preserve the high relaxivity and the target selectivity, the supramolecular aggregates should remain in a compact-defined structure during the imaging analysis. The aggregates should not collapse upon 1000–10,000-fold dilution once the stock solution of the contrast agent is injected in the human body. Concerning this issue, the use of micelles, especially those that are based on single-tailed amphiphilic monomers that give aggregates with high cmc, could be inappropriate. An alternative approach to prepare physiologically stable aggregates, that do not disaggregate even at high dilution, include the use of polymerized nanoparticles. They could be obtained by using polymerizable amphiphilic monomers: 10,12-pentacosadiynoic acid (PDA)-DTPAGlu(Gd) and PDA-L2-CCK8 contain the PDA as hydrophobic moiety, with two C≡C triple bonds, that can be irradiated by UV light to induce chain–chain polymerization in stable, covalently bound, aggregates [72]. These systems show an improved physical stability, originated from the increased rigidity and were able to avoid, to some extent, RES uptake. Aggregates obtained by mixing together PDA-DTPAGlu, or its Gd(III) complex, and PDA-L2-CCK8 in a 70:30 molar ratio before and after UV polymerization have been structurally characterized by means of SANS. Micelle aggregates have quite an elongated shape (with the axes ratio ranged between 2 and 3), and dimensions of semiaxis ranged between 10 and 30 Å; relaxivity value for each Gd complex, measured at 20 MHz and 298 K, are approximately 12 $mM^{-1}s^{-1}$.

### ■ Second-class naposomes

The possibility of using Gd-labeled micelles for imaging applications or as general micelles for drug delivery, depends on the degree of stability in the body of the aggregate loaded with the drug or with the contrast agent, relative to the cmc. The first class of naposomes is based on micelles obtained by co-assembling monomers with only one hydrophobic chain. Upon dilution in the blood following injection, these aggregates may not be sufficiently stable and disassemble immediately following administration. Hence, there is a need to find a new class of surfactant molecules able to form more stable aggregates, for example micelles with lower cmc values, or stable liposomes.

The second class of naposomes is based on amphiphilic monomers containing the peptide or the chelating agent bound to two hydrocarbon chains as the hydrophobic moiety **(FIGURE 6)**. These double-tailed monomers could give more stable nanoparticles; moreover, while single-chain monomers could disrupt biological membranes giving strong hemolytic effects, monomers bearing two hydrophobic tails, do not present hemolytic effects and toxicity problems due to their higher similarity with membrane phospholipids with respect to single-chain amphiphiles [101].

We reported supramolecular aggregates, basically constituted by an amphiphilic monomer in which the chelating agent (DTPAGlu, DTPA or DOTA) moiety is bound to a hydrophobic double-tail, with each hydrocarbon chain with 18 carbon atoms. The amphiphilic molecule $(C18)_2$DTPAGlu, as free base or as Gd complex, behaves as an anionic surfactant, and extruded at physiological pH, self-assembles in different aggregates (micelles with an elongated shape, and open bilayers, that could form stable liposomes) [65]. Variation of pH has a drastic effect on the size distribution of the aggregates: a micelle-to-vesicle transition is observed by decreasing the pH value from 7.4 to 3.0. In detail, micelle formation occurs in the pH range between 7.4 and 5.0, owing to the high negative charge of the surfactant headgroup, which causes strong headgroup–headgroup repulsions. A decrease of the pH (5.0–4.5) causes a protonation of the carboxylic functions and a decrease of the electrostatic repulsion between the headgroups, favoring the

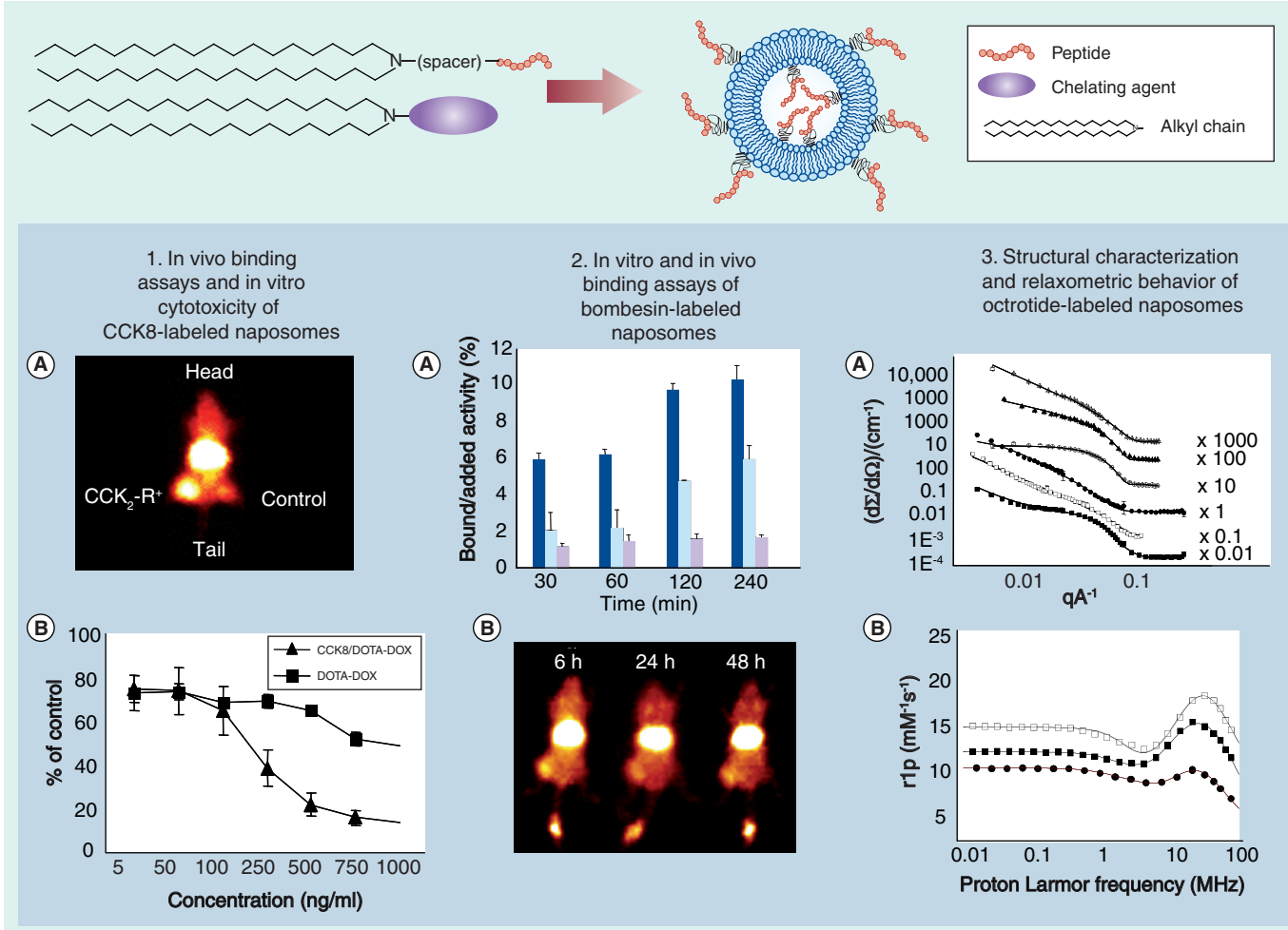


**Figure 6. Second class of naposomes, based on double-tailed monomers.** The upper side of the figure shows a schematic representation of the single monomers and of liposomes obtained by sonication and extrusion procedures. The lower shaded part of the figure shows selected results from structural and biological studies of naposomes labeled by CCK8 (1), bombesin (BN) (2) and octreotide (3) peptides. CCK8: **(1A)** γ-camera image (dorsal view) obtained prior to dissection of one of the animals 18 h after injection of radiolabeled aggregates clearly shows higher concentration of the radiolabel in the receptor positive xenograft (+, left flank) compared with the control tumor (-, right flank). These differences were statistically significant when comparing data from the five animals (paired t-test, p = 0.01). **(1B)** Cytotoxicity of liposomal doxorubicin (DXR) against human carcinoma cells. A431 cells were incubated with CCK8/DOTA-DXR and DOTA-DXR at different concentration ranging between 0 and 1000 ng/ml at 37°C. After 8 h, the medium was removed and after additional 72 h, an MTT assay was performed. BN: **(2A)** *In vitro* binding assays on PC-3 cell lines overexpressing the GRP at 37°C, at different time points of $^{111}$In-$(C18)_2$DOTA /$(C18)_2L_5$- [7-14] BN (90/10) (dark blue bars) with respect to the corresponding aggregates in which the BN peptide is replaced by the BN scrambled peptide (light blue bars) and to the self-assembled $^{111}$In-$(C18)_2$DOTA (gray bars). **(2B)** γ-camera images (ventral view) at different times after injection of $^{111}$In-$(C18)_2$DOTA/$(C18)_2L_5$ [7-14] BN naposomes. octreotide: **(3A)** Scattering cross sections of $(C18)_2$DTPAGlu(Gd)/$(C18)_2L_5$-Oct (■); $(C18)_2$DTPA(Gd) /$(C18)_2L_5$-Oct (□) and $(C18)_2$DOTA(Gd)/$(C18)_2L_5$-Oct (•) obtained at 25°C from small-angle neutron scattering experiments; **(3B)** NMR dispersion profiles of $(C18)_2$DTPAGlu(Gd)/$(C18)_2L_5$-Oct (□), $(C18)_2$DTPA(Gd)/$(C18)_2L_5$-Oct (■) and $(C18)_2$DOTA(Gd) /$(C18)_2L_5$-Oct (•) at pH = 7.4 and 298 K, normalized to 1-mM concentration of Gd(III) ion.

formation of thread-like micelles. Finally at pH 3, where all carboxylic groups are fully protonated, the formation of large, low curvature aggregates such as bilayer structures or liposomes is promoted. The effect of ionic strength on the systems of $(C18)_2$DTPAGlu in the absence and in presence of Gd(III) has been investigated at pH 7.4. In both cases any substantial effect of sodium chloride salt addition has not been revealed. Relaxivity values of $(C18)_2$DTPAGlu(Gd) aggregates at pH 7.4 in the presence and absence of sodium chloride at physiological ionic strength are 21.5 and 24.0 $mM^{-1}s^{-1}$, respectively.

Similar behavior has been found in the case of amphiphilic monomers containing DTPA or DOTA chelating agents, even if the negative charges diminish, going from five for DTPAGlu to four for DTPA and three for DOTA. After

Gd complexation, DTPA- and DOTA-chelating agents keep one and zero residual charges, respectively. Similarly to the pH effect observed for DTPAGlu, in this case a progressive decrease of the negative charges in the surfactant headgroup lead to a decrease of the electrostatic repulsion, favoring the formation of bilayer structures or liposomes [77].

In order to prepare target-selective nanoparticles, mixed supramolecular aggregates have been developed by adding a small amount of peptide-containing amphiphilic monomer. Several peptide monomers, in which three different bioactive sequences (CCK8, 7-14-BN or octreotide) and spacers of different length between the peptide and the alkyl chains have been used. The spacer length represents a critical point, in fact, as mentioned previously, the spacer should be long enough to assure an efficient exposure of the peptide beyond the surface of the aggregates and reduce potential hindrance to its specific binding activity, and at the same time, short enough to promote liposome formation.

Second-class naposomes labeled by CCK8 peptide were prepared by starting from three peptide monomers: one in which the spacer consists of five units of ethyleneglycol, $(C18)_2L_5CCK8$ [66,68,71], one in which the spacer is a PEG chain with an average molar weight of 2000 g $mol^{-1}$ ($PEG_{2000}$), $(C18)_2PEG_{2000}CCK8$ [70] and one containing the DSPE–$PEG_{2000}$ moiety (DSPE–$PEG_{2000}$-CCK8) [67].

$(C18)_2L_5CCK8$, is able to self-assemble spontaneously in well-ordered nanostructures in aqueous solution [102] and characterized by water-exposed CCK8 peptide in β-sheet conformation. They are able to encapsulate anticancer drugs such as DOX, and could be employed for target-selective drug delivery on a biological target, through the bioactive peptide exposed on the external surface.

Mixed aggregates $(C18)_2$DTPAGlu(Gd)/$(C18)_2L_5CCK8$ (70:30 monomer ratio) are characterized by the presence of bilayer structures (open bilayers and liposomes) under physiologic conditions [68]. The relaxivity value of each Gd complex in liposomes (hydrodynamic radius of ~300 Å) was of approximately 21.0 $mM^{-1}s^{-1}$. This relaxivity value represents the sum of both inner and outer Gd complexes because of the high membrane water permeability [66]. Similar relaxivity behavior has been obtained for aggregates in which the $(C18)_2L_5CCK8$ monomer is replaced by $(C18)_2PEG_{2000}CCK8$. From a structural point of view, mixed aggregates based on CCK8 peptide ($[C18]_2$DTPAGlu/$[C18]_2PEG_{2000}CCK8$) in a 70:30 ratio, appear in solution as a combination of rod-like micelles (radius of ~40 Å and length >700 Å), open bilayer fragments (thickness ~65 Å) and liposomes [70]. Therefore, when the $L_5$ spacer is replaced by $PEG_{2000}$, there is an increase in micelle population:PEG-containing monomers, which also show a lower tendency to form liposomes in comparison with L5-containing monomers after sonication and extrusion processes.

Stable lamellar aggregates were obtained in the case of samples containing only DSPE–$PEG_{2000}$–CCK8, or a quantity of $(C18)_2$DTPAGlu(Gd) up to 50% [67]. By increasing the amount of $(C18)_2$DTPAGlu(Gd) in the aggregate, a lamellar aggregates-to-rod-like micelle transition is observed. This structural transition can probably be attributed to the presence of the uncharged peptide monomer that interposes between the charged headgroups of the chelating agent monomer. The proton relaxivity was exactly the same (17.2 $mM^{-1}s^{-1}$) for both lamellar aggregates and rod-like micelles though in the two cases its value is the result of the combination of different local and global contributions.

*In vitro* and *in vivo* selective binding activity and biodistribution of mixed aggregates derivatized by CCK8 were studied by nuclear medicine experiments [70]. For this purpose the Gd ion was replaced with a $^{111}$In γ-emitting radioisotope, as reported above for first-class naposomes. Mixed aggregates based on the CCK8 peptide ($[C18]_2$DTPAGlu/$[C18]_2Peg_{2000}CCK8$ in a 70:30 ratio) that appear in solution as a combination of rod-like micelles, open bilayer and liposomes, present the CCK8 bioactive peptide well exposed on the external aggregate surface, as indicated by fluorescence measurements [70]. This feature should make possible the selective target of these nanocarriers towards the cholecystokinin receptors overexpressed by the cancerous cells. In fact, $^{111}$In-labeled aggregates show preferential binding to A431 cells overexpressing the $CCK_2$-R by transfection compared with control cells both at 4°C and at 37°C. *In vivo* biodistribution experiments show that overall retention of the radiolabel in the experimental animals at 18 h is very high, with essentially no excretion of the starting radioactivity over the observation period. All organs show significant retention of radioactivity, although this is particularly elevated in organs with a RES such as the liver and spleen. Direct comparisons, within the same animal of the biodistribution data show that

receptor-positive xenografts were always higher in radioactivity retention than their respective controls. The average enrichment factor in radioactivity of the $CCK_2$-R positive xenografts was found to be 48 ± 21% **(FIGURE 6.1A)** Any acute toxicity following the intravenous administration of the compound is observed during the observation period. Moreover, the drug loading capability of the aggregates and their drug efficiency on the target cells was reported by using the cytotoxic DOX drug. Incubation of receptor positive and control cells with peptide-containing aggregates filled with DOX showed significantly lower cell survival in receptor-expressing cells with respect to the control, for samples incubated in the presence of DOX. Comparable results were obtained with mixed liposomes, prepared by combining together, in a 90:10 molar ratio, $(C18)_2$DOTA–$(C18)_2L_5$CCK8. The DOX loading content was above 95% of the total drug and the corresponding drug:lipid w/w ratio was 0.134. The cellular uptake of the targeted liposomal DOX CCK8–DOTA-DOX with respect to the self-assembled, nonspecific, liposomal DOX DOTA-DOX has been evaluated by the use of flow cytometry assays **(FIGURE 6.1B)**. The cell-associated DOX on A431 and HUVEC cells for peptide-derivatized liposomes was 70- and 8-fold higher than that for nontargeted liposomes, respectively, indicating that the bioactive CCK8 peptide is able to enhance the DOX uptake into the A431 carcinoma cells and, to a lower extent, in the endothelial HUVEC cells. Cells incubated with peptide-derivatized liposomes showed significantly lower cell survival compared with nontargeted liposomes, in the presence of drug amounts ranging between 250 and 1000 ng/ml [74].

*In vitro* and *in vivo* binding assays by nuclear medicine were also carried out on second-class naposomes based on (7-14)-BN peptide ($[C18]_2$DOTA/$[C18]_2$-spacer-[7-14]-BN) [75]. The peptide in the amphiphilic monomer is spaced by the lipophilic moiety through ethoxylic spacers of different length: a shorter spacer with five units of dioxoethylene moieties in $(C18)_2L_5$-peptide, or a longer spacer consisting of a $PEG_{3000}$ residue in $(C18)_2PEG_{3000}$-peptide. Structural characterization by SANS and dynamic light scattering (DLS) techniques indicate that, independently from the amount (<10%) of the peptide-containing monomer in the final composition, the predominant aggregates are liposomes of similar shape and size with a hydrodynamic radius $R_h$ of approximately 200 nm and bilayer thickness, *d*, of 4 nm. This structure is slightly different from that observed for CCK8 aggregates described above in which DTPAGlu amphiphilic monomer is present, and highly polydisperse aggregates are found. This behavior could be explained on the basis of the lower negative charge (-3) of DOTA with respect to DTPAGlu (-5). *In vitro* data, reported in **FIGURE 6.2A**, show specific binding of the $^{111}$In-$(C18)_2$DOTA–$(C18)_2L_5$-(7-14) BN-containing aggregates in receptor-expressing cells. Instead, the presence of PEG3000 units on the external liposomal surface, could hide the peptide and prevent the receptor binding. In fact, too high a surface coverage could be unfavorable for targeting purposes, since it may prevent the contact between the peptide and the membrane receptors [75].

*In vivo* experiments using $^{111}$In-$(C18)_2$DOTA/$(C18)_2L_5$-(7-14)-BN show the expected biological behavior of aggregates of such size and molecular composition preliminarily confirm the ability to specifically target and concentrate in receptor expressing xenografts **(FIGURE 6.2B)**. In fact it can be observed that an increase in concentration of the targeting agent aggregate in the tumors compared with controls, at the 48 h time point evaluated (2.4% ID/g vs 1.6% ID/g).

Second-class naposomes based on an octreotide peptide were also prepared as diagnostic tools in MRI [77]. They present high relaxivity values typical of the new generation of MRI contrast agents, based on nanoparticles obtained by lipophilic Gd(III) complexes [103,104]. Naposomes were formulated by mixing two amphiphilic monomers. The first monomer $(C18)_2L_5$-Oct contains two C18 hydrophobic moieties bound to the N-terminus of the cyclic peptide octreotide, and spaced from the bioactive peptide by five units of dioxoethylene linkers, while the second monomer is $(C18)_2$DTPAGlu or $(C18)_2$DTPA or $(C18)_2$DOTA. The number of oxoethylene linkers was selected, according to biological results previously obtained on similar aggregates derivatized with CCK8 [70] or 7-14-BN [75], in order to favor a good exposure of octreotide on the external aggregate surface. The presence of a small amount of amphiphilic octreotide monomer exposed on the aggregate surface, as indicated by fluorescence studies, give the nanoparticles a potential binding selectivity toward the somatostatin SSTR2 receptor subtype. Structural differences between the aggregates formulated by starting from the three chelating agents, or from their Gd complexes, have been observed and rationalized by

SANS measurements, on the basis of their different residual charge **(FIGURE 6.3A)**. According to other reported systems [65], a decrease of the negative charges on the aggregate surface promotes a micelle-to-vesicle transition going from two for DTPAGlu(Gd) to one for DTPA(Gd) and zero for DOTA(Gd). A decrease in relaxivity values (from $r_{1p}$ = 17.6–10.0 $mM^{-1}s^{-1}$), due to an increase of water exchange lifetimes ($\tau_M$) of the monoamides, can be observed in **FIGURE 6.3B** going from $(C18)_2$DTPAGlu(Gd)- to $(C18)_2$DOTA(Gd)-containing ternary systems.

## ■ Third-class naposomes

A further upgrade of the naposomes supramolecular system is obtained by designing and synthesizing new monomers with an 'upsilon' shape and indicated as *MonY* **(FIGURE 7)**. This monomer combines in the same molecule all the three fundamental tasks that are required to obtain target-selective nanoparticles for delivery of drugs and contrast agents:

- The bioactive peptide;
- The chelating agent;
- The hydrophobic moiety;

The *MonY* monomer is based on a lysine residue derivatized on its three reactive functions with:

- DTPAGlu or DOTA chelating agent on the side-chain ε-amino group;
- CCK8 or octreotide peptide on the lysine carboxylic function;
- The hydrophobic moiety containing two 18 carbon-atom alkyl chains on the lysine α-amino group [69,76].

DTPAGlu was selected as chelating agent in CCK8-*MonY* monomer [69], while DTPAGlu and DOTA were chosen for octreotide-*MonY* [76]. According to DLS and SANS data, *MonY* molecules are always able to form ellipsoidal micelles and bilayer structures when in their uncomplexed form. On the contrary, monomers based on DOTA are not able to self-aggregate when complexed with Gd(III) ions. The complete loss of charges on the Gd–DOTA complex produces a remarkable reduction of the anionic character of the amphiphilic monomer, which is no longer able to aggregate.

The two CCK8-*MonY* and octreotide-*MonY* based on DTPAGlu chelating agent, self-aggregate in buffered water solution giving ellipsoidal micelles in which the ratio between micelle axes is approximately 2.7 and the aggregation number $N_{agg}$ is approximately 30 **(FIGURE 7).** There were no detectable differences in the aggregation behavior between *MonY* and *MonY*(Gd), indicating that the presence of metal ions, and therefore the reduction of the net charge, does not substantially influence the aggregation behavior. Aggregate shape and size of the two *MonY* are similar to micelles obtained by co-aggregation of two monomers, one bearing the Gd complex and the other the bioactive peptide, and both containing one single hydrocarbon C18 chain (first-class naposomes). The ellipsoidal rather than the spherical shape of the previously reported system is the most evident structural difference; moreover the presence of the double hydrocarbon chain gives higher micelle stability in water solution as indicated by lower cmc values. In the case of aggregates obtained by using CCK8-*MonY*, fluorescence studies and circular dichroism experiments indicate the complete exposure of CCK8 peptide on the micelle surface, and the predominant presence of an antiparallel β-sheet peptide conformation characterized by a β-like turn. The high relaxivity values of CCK8-*MonY* and octreotide-*MonY* micelles ($r_{1p}$ = 15.0 $mM^{-1}s^{-1}$ and $r_{1p}$ = 13.9 $mM^{-1}s^{-1}$ at 20 MHz and 25°C, respectively), indicate these aggregates as promising target-selective MRI contrast agents.

In order to obtain multimodal liposome aggregates for simultaneous drug and contrast agent delivery, *MonY* has been mixed with dioleoylphosphatidylcholine (DOPC), a phospholipid that is one of the main lipids composing the cell membrane. DOPC self-assembles in liposomes and these structures preserve shape and characteristics on addition of *MonY* or *MonY*(Gd) up to an amount of 20% of the total concentration [69]. The thickness of the liposome bilayer is measured by SANS to be 30–40 Å, whereas cryo-transmission electron microscopy images show that the liposome diameter ranged between 50 and 150 nm (**FIGURE 7;** right). Upon raising the amount of *MonY*, in the mixed aggregated to 50%, the liposome structures are destabilized leading to bilayers that coexist with rod-like micelles, as indicated by scattering techniques. Relaxivity values of each Gd complex in DOPC–*MonY*(Gd) liposomes (80:20 in molar ratio) is 12.7 $mM^{-1}s^{-1}$, at 20 MHz and 25°C.

As reported in **FIGURE 7** aggregates belonging to the third class of naposomes have been tested for their targeting behavior. Results obtained by γ-counts on A431 cells and compared with control cells after incubation with third-class

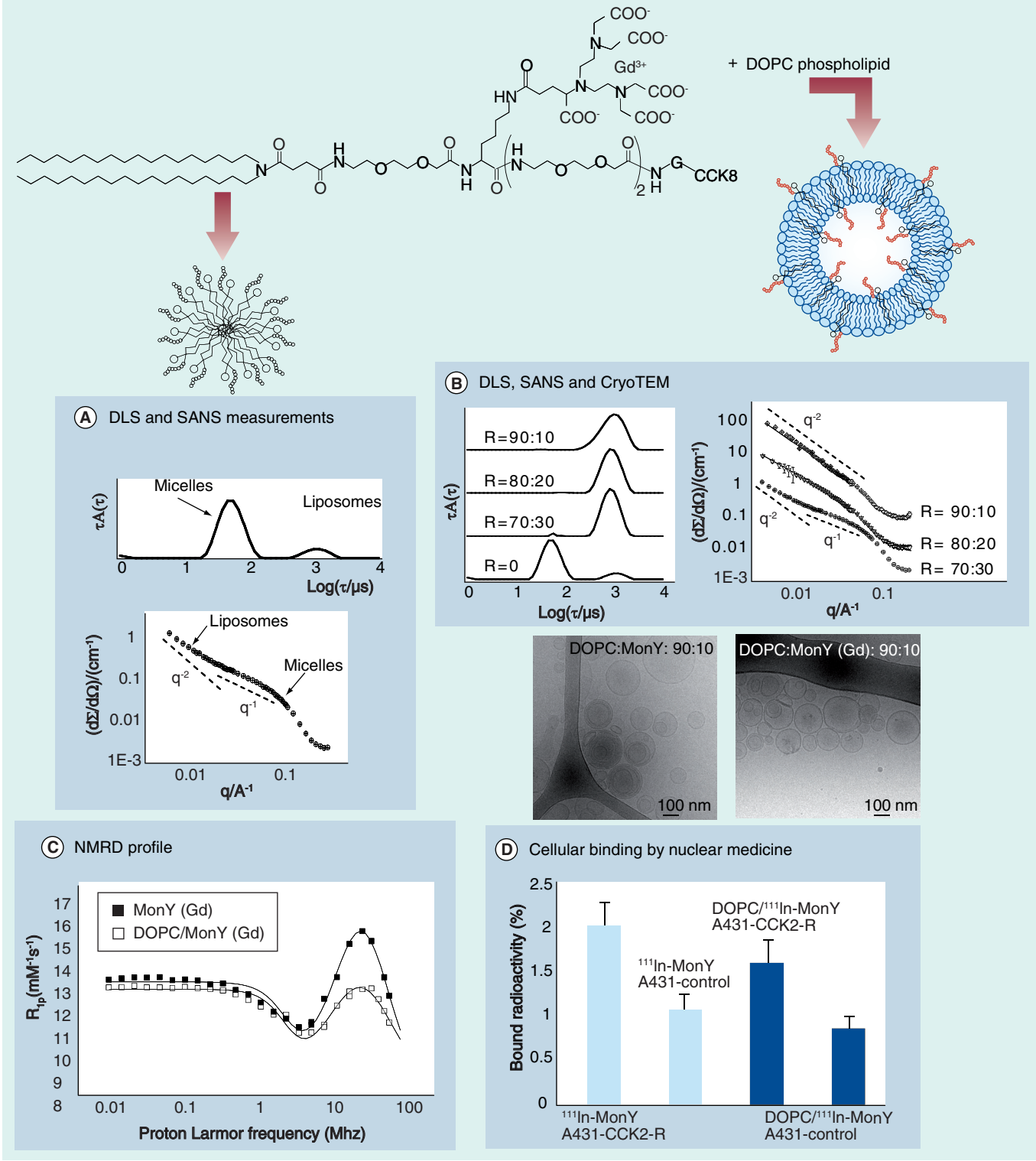


**Figure 7. Third-class naposomes, based on monomers with an upsilon shape (*MonY*).** The upper figure shows the chemical structure of the *MonY*(Gd) monomer. Middle: **(A)** representation and the structural characterization (relaxation time distributions at q = 90° and scattering cross-section at 25°C) of self-assembled aggregates based on *MonY*(Gd) (left side); **(B)** representation and the structural characterization (relaxation time distributions at q = 90°, scattering cross-sections, and selected cryo-TEM images) of mixed aggregates of DOPC/*MonY*(Gd) at several molar ratios (right). Bottom: **(C)** NMR dispersion profiles of *MonY*(Gd) (■) and DOPC-MonY(Gd) (80:20) (□) at pH 7.4 and 25°C, normalized to 1 mM concentration of Gd(III) ion (left); **(D)** binding of $^{111}$In-labeled nanoparticles to A431 cells overexpressing CCK2-R, compared with control cells (right). DLS: Dynamic light scattering; DOPC: Dioleoylphosphatidylcholine; SANS: Small-angle neutron scattering; TEM: Transmission electron microscopy.

naposomes labeled with the $^{111}$In indicate target selectivity both for micelles obtained by self-assembling *MonY* and for mixed liposomes containing 20% of *MonY* in DOPC.

### ■ Fourth-class naposomes

Fourth-class naposomes are based on 'gemini' surfactants. In general, gemini surfactants are formed by the covalent linking of two 'conventional' surfactants via a spacer. These surfactants have interesting features, such as low cmc values, which drastically reduce cytolytic action on the cell membrane [105,106]. By manipulating the molecular architecture and the solution conditions, a variety of supramolecular aggregates, such as micelles and liposomes, can be obtained. According to the naposomes strategy, two gemini surfactants have been developed [73]: the first one containing the bioactive sequence of the cholecystokinin peptide CCK8[C18CysL$_5$CCK8]$_2$ and the second one containing the chelating agent DTPAGlu or its Gd complex, DTPAGlu(Gd), [C18CysDTPAGlu(Gd)]$_2$ **(FIGURE 8)**. Gemini surfactants were easily synthesized in the solid phase by introducing a cysteine residue in the peptide sequence. The presence of the cysteine residue in the sequence allows disulphur-bridge formation under mild oxidative conditions, reducing the purification steps. The supramolecular aggregates obtained by co-assembling of the two synthetic gemini surfactants, at a 70:30 molar ratio between chelating agent-containing gemini surfactant, or its corresponding Gd(III) complex, and peptide gemini surfactant, have been structurally identified as cylindrical or ellipsoidal micelles (**FIGURE 8**, curly brackets). These mixed aggregates represent the first example of peptide-containing gemini surfactants as potential target-selective contrast agents in MRI. The cmc values indicate that all monomers in aqueous solution aggregate at the molar concentration in the $5{\cdot}10^{-6}$–$1{\cdot}10^{-5}$ mol/Kg$^{-1}$ range. These values are only slightly lower than cmc values for the first class of naposomes ($5{\cdot}10^{-5}$ mol/Kg$^{-1}$) and slightly higher than those found for second class amphiphiles ($5{\cdot}10^{-7}$ mol/Kg$^{-1}$). Hence, gemini compounds present two different effects: the higher tendency to aggregate with respect to the mono-tailed monomers, and the higher electrostatic repulsion between the two head groups due to the negative charges of DTPAGlu moieties. On the contrary, the cmc value (~$6{\cdot}10^{-6}$ mol/Kg$^{-1}$) found for [C18CysL$_5$CCK8]$_2$ monomer, in which there are no repulsion effects, is in agreement with the low expected values for gemini surfactants. In fact, the corresponding mono-tailed monomer (C18L$_5$CCK8) did not show any tendency to aggregate in the same experimental conditions. Moreover, fluorescence spectroscopy confirmed the presence of the bioactive peptide well exposed on the aggregate external surface: fluorescence emission at approximately 360 nm of the tryptophan indole moiety is indicative of the presence of tryptophan residue in a polar aqueous solvent, suggesting the presence of the entire CCK8 peptide on the micellar external environment.

As expected for short peptide sequences the CCK8 octapeptide moiety does not undergo any folding process in a water solution. On the other hand, in micelle aggregates obtained by self-assembling of (C18)$_2$L$_5$CCK8, the peptide shows a classical β-sheet fold. This result suggests that the hydrogen bonds among amino acids, well exposed on the external surface of the aggregates, promote intermolecular sheet-like structures that are stabilized by interactions between the alkyl chains. In the present case, according to the previous results, the circular dichroism spectrum of [C18CysL$_5$CCK8]$_2$ reveals the characteristic shape of a β-sheet-type structure. Upon heating the solution, the intensity of the circular dichroism spectra of the β-sheet structure signals (222 nm), decreases linearly, suggesting the breaking up of the interactions between nearer peptides. By plotting the intensity of the circular dichroism spectra at 222 nm as a function of temperature, a sigmoid curve is observed. The maximum in the first derivative of the sigmoid curve indicates the transition temperature ($T_t$ ~45°C) in which the peptide structure changes from a β-sheet to a random coil structure. The same result is observed for mixed aggregates in which DTPAGlu is present as free base or as Gd complex, indicating that, CCK8 molecules notwithstanding, their dilution in (C18CysDTPAGlu)$_2$ aggregates, are still close enough to each other to maintain hydrogen bonds among peptide chains **(FIGURE 8A)**. The shape and size of pure and mixed aggregates are also influenced by the temperature: at lower temperatures micelle aggregates have elongated shapes with a cylindrical structure, while at higher temperatures ellipsoidal shapes are found **(FIGURE 8B)**. It seems that the increase of the temperature leads to progressive shortening of the cylindrical structures up to ellipsoidal micelles. Likewise, the surface-exposed CCK8 peptide changes its conformation by increasing the

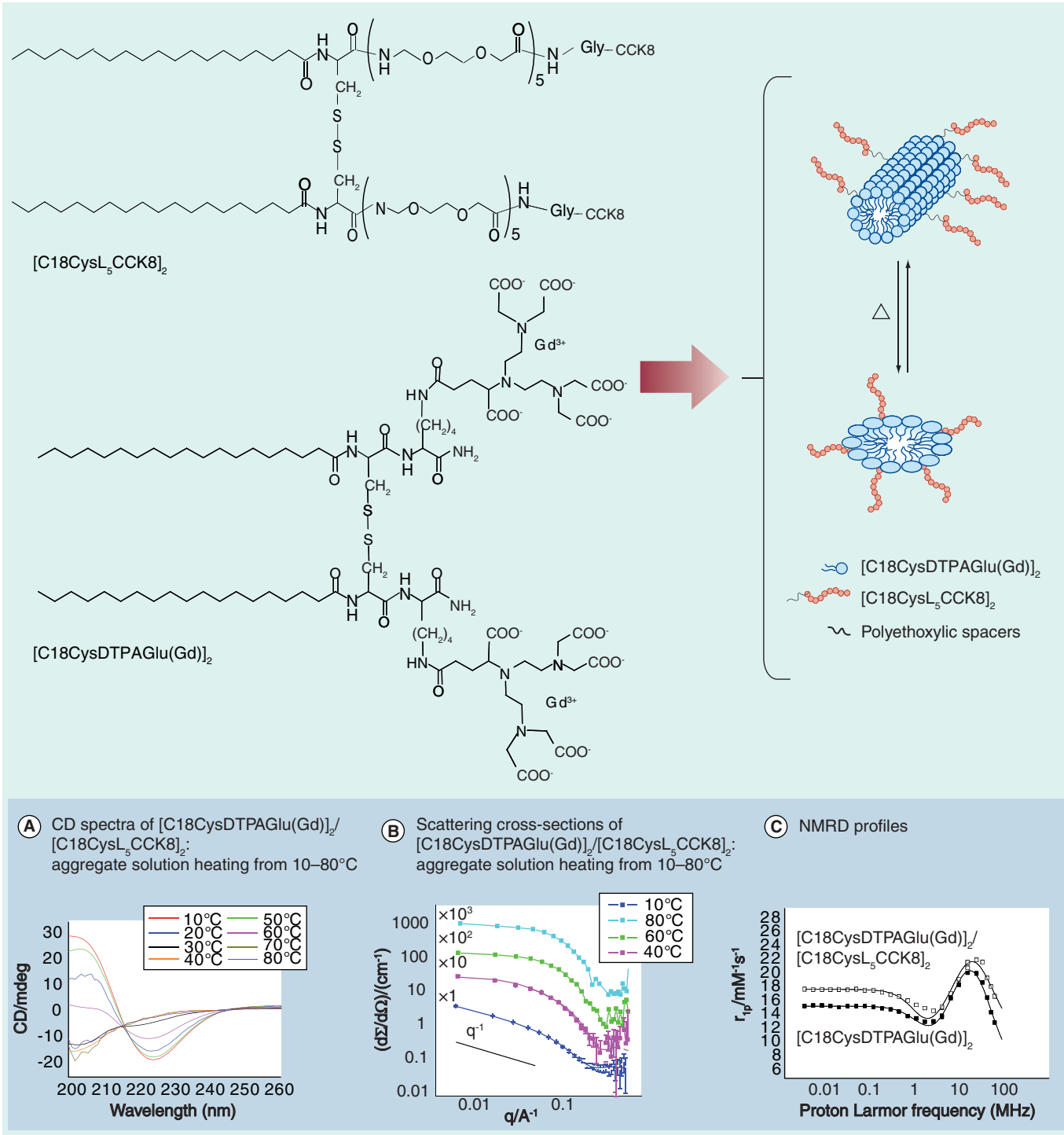


**Figure 8. Fourth-class naposomes, based on Gemini surfactants.** The upper part of the figure shows a representation of $[C18CysDTPAGlu(Gd)]_2$ and $[C18CysL_5CCK8]_2$ gemini amphiphilic monomers, obtained by connecting two identical moieties by a disulphide bond. In the curly brackets is a schematic representation of the $[C18CysDTPAGlu(Gd)]_2/[C18CysL_5CCK8]_2$ aggregates (70:30 molar ratio); their shape is temperature dependent. In the bottom side of the panel is reported the structural characterization and relaxometric behavior of the $[C18CysDTPAGlu(Gd)]_2$–$[C18CysL_5CCK8]_2$ system (pH 7.4, 1·10–4M concentration of the gemini peptide is reported): **(A)** circular dichroism spectra of aggregate solution recorded in the 10–80°C range; **(B)** Scattering cross-sections measured heating up aggregates at the temperatures reported in the legend. Cross-sections have been multiplied for a scale factor, as indicated; **(C)** NMR dispersion profiles recovered at 25°C, normalized to 1 mM concentration of Gd(III) ion.

temperature, going from a β-sheet to a random coil structure. Even if there is any evidence that the two phenomena are related, the similarity of the transition temperatures of the two processes, as well as the amplitude of the hysteresis indicate a possible co-operation between the aggregate structure transition and the peptide conformation variation. In **Figure 8C** the relaxivity values of pure and mixed micelles at 25°C (18.4 and 21.5 $mM^{-1}s^{-1}$, respectively) are reported. These values are in accordance with the other classes of naposomes and with other Gd-containing micelle systems, as almost all the q = 1 (one inner-sphere water molecule) Gd-based micelles have relaxivity values in the range 18–23 $mM^{-1}s^{-1}$ (20 MHz; 25°C) for each Gd atom.

## Future perspective

Biological tests of naposomes show properties that appear potentially suitable for clinical applications: significantly higher concentration of aggregates in receptor-expressing xenografts relative to controls has been established *in vivo*, suggesting that these aggregates may be utilized to increase concentration of the Gd MRI contrast agent and/or of a drug, to cells expressing a specific receptor target.

Slow plasma kinetics with prolonged half-life and low breakdown of the supramolecular aggregates, both probably due to the presence of PEG moieties on the aggregate external surface, appear useful for maintaining high blood concentrations of the delivered compound.

The long circulation times, the elevated specific targeting properties of the aggregates and their selective cytotoxic efficiency on the target cells, are in line with the desired pharmacokinetic properties of a drug-delivery nanovector.

These results indicate that naposomes, in which CCK8, 7-14-BN, or octreotide peptides are exposed on the external aggregate surface, could efficiently act as target-selective tools for delivery of a contrast agent (paramagnetic Gd complexes for MRI, or radioactive metal ions for MRI or scintigraphic images, respectively) and/or drugs to cancer cells overexpressing specific membrane receptors. By combining the contrast agent and the drug in the same nanoparticle, naposomes represent efficiently theradiagnostic systems.

The development of naposome lead compounds containing the BN peptide on their external surface for imaging and therapeutic application in ovarian cancer is in progress. The first Phase 1 clinical studies are scheduled for coming years.

## Executive summary

- New supramolecular aggregates – termed naposomes – with shapes and sizes that can be modulated at will, containing chelating agents and bioactive peptides and acting as effective and selective delivery tools for drug and/or contrast agents have been developed in recent years. They represent a new generation of theradiagnostic nanoparticles.
- Naposomes are supramolecular aggregates (micelles, vesicles or liposomes) obtained by coaggregation of two monomers: a first monomer containing a chelating agent that is able to coordinate a radioactive or paramagnetic metal ion and having a lipophilic moiety, and a second monomer containing a bioactive peptide linked to a similar lipophilic moiety.
- The aggregates are selectively driven by the exposed bioactive peptide on the chosen biological target. Oxo-ethylene moieties (polyethylene glycol units) are introduced to space the bioactive peptide from the aggregate external surface and to improve the *in vivo* permanence of the aggregates.
- The aggregates are able to entrap in their inner compartment or in the phospholipid bilayer, a pharmaceutical active principle, for example the cytotoxic drug doxorubicin (DOX).
- Four different classes of naposomes, based on the combination of different monomers, are discussed. The bioactive peptides exposed on their external surface are: CCK8, 7-14-bombesin and octreotide.
- The innovative aspects related to naposomes, with respect to liposomal drugs already in use (Myocet®, liposomial DOX and DOXIL® polyethylene glycolhilated liposomal DOX), concerns the presence of the bioactive peptides well exposed on the aggregate external surface, which allows selective delivery to cancer cells overexpressing membrane receptors for the bioactive peptide. Moreover, the presence of the chelating agent allows the aggregates to achieve several goals according to the complexed metal ion.
- Effective and selective drug-delivery systems containing a marker that is able to monitor the *in vivo* circulation and the *in vivo* biodistibution of the drug-containing aggregate can be achieved by using nuclear medicine techniques if the metal is represented by a γ-emitting ($^{111}$In, $^{99m}$Tc[V] or $^{67}$Ga[III]) isotope.
- Naposomes have a high relaxivity and are target-selective contrast agents for MRI application.
- Naposomes are an effective and selective drug-delivery system, and a powerful radiotherapeutic compound containing, simultaneously, a drug entrapped in the inner compartment of the aggregate and a β-emitting radioactive metal ion ($^{90}$Y[III] or $^{177}$Lu[III]) complexed by the chelating agent.

## Acknowledgements

*The authors are indebted to Luigi Aloj, Nuclear Medicine Department, Cancer Institute 'G. Pascale', Napoli, Italy, for his high contribution to naposomes development from a medical point of view, and to Luigi Paduano, Department of Chemistry, University of Naples 'Federico II', Italy, for his collaboration in naposomes structure identification.*

## Financial & competing interests disclosure

*The authors have participation and financial interest in a spin-off company, Invectors srl, devoted to the clinical development of the described compounds for cancer therapy. The authors have no other relevant affiliations or financial involvement with any organization or entity with a financial interest in or financial conflict with the subject matter or materials discussed in the manuscript apart from those disclosed.*

*No writing assistance was utilized in the production of this manuscript.*

## Bibliography

Papers of special note have been highlighted as:
- ▪ of interest
- ▪▪ of considerable interest

1 Gregoriadis G, Ryman BE. Lysosomal localization of fructofuranoside-containing liposomes injected into rats. *Biochem. J.* 129, 123–133 (1972).

2 Maeda H, Wu J, Sawa T, Matsumura Y, Hori K. Tumor vascular permeability and the EPR effect in macromolecular therapeutics: a review. *J. Control. Release* 65, 271–84 (2000).

3 Bajoria R, Contractor SF. Effect of surface charge of small unilamellar liposomes on uptake and transfer of carboxyfluorescein across the perfused human term placenta. *Pediatr. Res.* 42, 520–527 (1997).

4 Miller CR, Bondurant B, McLean SD, McGovern KA, OBrien DF. Liposome-cell interactions *in vitro*: effect of liposome surface charge on the binding and endocytosis of conventional and sterically stabilized liposomes. *Biochemistry* 37, 12875–12883 (1998).

5 Nakanishi T, Kunisawa J, Hayashi A *et al.* Positively charged liposome functions as an efficient immunoadjuvant in inducing immune responses to soluble proteins. *Biochem. Biophys. Res.Commun.* 240, 793–797 (1997).

6 Scherphof GL, Kamps JA. Receptor versus nonreceptor mediated clearance of liposomes. *Adv. Drug Deliv. Rev.* 32, 81–97 (1998).

7 Papisov MI. Theoretical considerations of RES-avoiding liposomes: molecular mechanics and chemistry of liposome interactions. *Adv. Drug Deliv. Rev.* 32, 119–138 (1998).

8 Bakker J, Sanders A, Van Rooijen N. Effects of liposome-encapsulated drugs on macrophages: comparative activity of the diamidine 4′,6-diamidino-2-phenylindole and the phenanthridinium salts ethidium bromide and propidium iodide. *Biochim. Biophys. Acta* 1373, 93–100 (1998).

9 Mayer LD. Future developments in the selectivity of anticancer agents: drug delivery and molecular target strategies. *Cancer Metastasis Rev.* 17, 211–218 (1998).

10 Sharma A, Sharma US. Liposomes in drug delivery: progress and limitations. *Int. J. Pharm.* 154, 123–140 (1997).

11 Boswell GW, Buell D, Bekersky I. AmBisome® (liposomal amphotericin B): a comparative review. *J. Clin. Pharmacol.* 38, 583–592 (1998).

12 Allen TM. Liposomes: opportunities in drug delivery. *Drugs* 54, 8–14 (1997).

▪▪ **Liposomal drug-delivery systems markedly alter biodistribution of associated drugs. This increases the drug therapeutic indices, by increasing the drug concentration in solid tumors and regions of infection, and reducing the drug concentration in normal tissues.**

13 Allen TM, Moase EH. Therapeutic opportunities for targeted liposomal drug delivery. *Adv. Drug Deliv. Rev.* 21, 117–133 (1996).

14 Bally MB, Nayar R, Masin D, Hope MJ, Cullis PR, Mayer LD. Liposomes with entrapped doxorubicin exhibit extended blood residence times. *Biochim. Biophys. Acta* 1023, 133–139 (1990).

15 Bandak S, Ramu A, Barenholz Y, Gabizon A. Reduced UV-induced degradation of doxorubicin encapsulated in polyethylene glycol-coated liposomes. *Pharm. Res.* 16(6), 841–846 (1999).

16 Coukell AJ, Spencer CM. Polyethylene glycol-liposomal doxorubicin: a review of its pharmacodynamic and pharmacokinetic properties, and therapeutic efficacy in the management of AIDS-related Kaposi's sarcoma. *Drugs* 53(3), 520–538 (1997).

17 Gabizon A, Goren D, Cohen R, Barenholz Y. Development of liposomal anthracyclines: from basics to clinical applications. *J. Control. Release* 53, 275–279 (1998).

▪ **The pharmacokinetic behaviour of polyethylene glycol-liposomal doxorubicin (DXR) shows an improved extravasation profile with enhanced localization in tumors and superior therapeutic efficacy in comparison with doxorubicin in free form.**

**In clinical studies, doxorubicin encapsulated in polyethylene glycol-coated liposomes shows a unique pharmacokinetic toxicity profile and promising antitumor activity.**

18 Batist G, Ramakrishnan G, Rao CS *et al.* Reduced cardiotoxicity and preserved antitumor efficacy of liposome-encapsulated doxorubicin and cyclophosphamide compared with conventional doxorubicin and cyclophosphamide in a randomized, multicenter trial of metastatic breast cancer. *J. Clin. Oncol.* 19, 1444–1454 (2001).

19 Shiraga E, Barichello JM, Ishida T, Kiwada H. A metronomic schedule of cyclophosphamide combined with PEGylated liposomal doxorubicin has a highly antitumor effect in an experimental pulmonary metastatic mouse model. *Int. J. Pharm.* 353, 65–73 (2008).

20 Soepenberga O, Sparrebooma A, de Jongea JA *et al.* Real-time pharmacokinetics guiding clinical decisions: Phase I study of a weekly schedule of liposome encapsulated paclitaxel in patients with solid tumors. *Eur. J. Cancer* 40, 681–688 (2004).

21 Mita M, Mita A, Sarantopoulos J *et al*. Phase I study of paclitaxel poliglumex administered weekly for patients with advanced solid malignancies. *Cancer Chemother. Pharmacol.* 64(2), 287–295 (2009).

22 Johnson EM, Ojwang JO, Szekely A, Wallace TL, Warnock DW. Comparison of *in vitro* antifungal activities of free and liposome-encapsulated nystatin with those of four amphotericin B formulations. *Antimicrob. Agents Chemother.* 42, 1412–1416 (1998).

23 Oakley KL, Moore CB, Denning DW. Comparison of *in vitro* activity of liposomal nystatin against *Aspergillus* species with those of nystatin, amphotericin B (AB) deoxycholate, AB colloidal dispersion, liposomal AB, AB–lipid complex, and itraconazole. *Antimicrob. Agents Chemother.* 43, 1264–1266 (1999).

24 Jessup C, Reyes G, Fothergill A *et al*. A head-on comparison of the *in vitro* antifungal activity of conventional and lipid-based amphotericin B: a multicenter study. *J. Chemother.* 12, 22–29 (2000).

25 Gondal JA, Swartz RP, Rahman A. Therapeutic evaluation of free and liposome-encapsulated amphotericin B in the treatment of systemic candidiasis in mice. *Antimicrob. Agents Chemother.* 33, 1544–1548 (1989).

26 Mayer LD, Harasym TO, Tardi PG *et al.* Ratiometric dosing of anticancer drug combinations: controlling drug ratios after systemic administration regulates therapeutic activity in tumor-bearing mice. *Mol. Cancer Ther.* 5, 1854–1863 (2006).

27 Wang J, Goh B, Lu W *et al. In vitro* cytotoxicity of stealth liposomes co-encapsulating doxorubicin and verapamil on doxorubicin-resistant tumor cells. *Biol. Pharm. Bull.* 28, 822–828 (2005).

▪ **Novel doxorubicin antiresistant stealth liposomes, prepared by co-encapsulating DOX and verapamil into stealth liposomes, have been developed. DOX antiresistant stealth liposomes were effective DOX formulations, which could overcome drug resistance in DOX-resistant tumor cells.**

28 Battistini E, Gianolio E, Gref R *et al.* High-relaxivity magnetic resonance imaging (MRI) contrast agent based on supramolecular assembly between a gadolinium chelate, a modified dextran, and poly-β -cyclodextrin. *Chem. Eur. J.* 14, 4551–4561 (2008).

29 Aime S, Botta M, Garino E *et al.* Noncovalent conjugates between cationic polyamino acids and GdIII chelates: a route for seeking accumulation of MRI-contrast agents at tumor targeting sites. *Chem. Eur. J.* 6(14), 2609–2617 (2000).

30 Tilcock C, Unger E, Cullis P, MacDougall P. Liposomal Gd-DTPA: preparation and characterization of relaxivity. *Radiology* 171(1), 77–80 (1989).

31 Kabalka G, Buonocore E, Hubner K, Moss T, Norley N, Huang L. Gadolinium-labeled liposomes: targeted MR contrast agents for the liver and spleen. *Radiology* 163(1), 255–258 (1987).

32 Grant CWM, Karlik S, Florio EA. A liposomal MRI contrast agent: phosphatidylethanolamine-DTPA. *Magn. Reson. Med.* 11(2), 236–243 (1989).

33 Unger E, Fritz T, Wu G *et al.* Liposomal MR contrast agents. *J. Liposome Res.* 4(2), 811–834 (1994).

34 Unger E, Shen DK, Wu GL, Fritz T. Liposomes as MR contrast agents: pros and cons. *Magn. Reson. Med.* 22(2), 304–308 (1991).

35 Koenig SH, Ahkong QF, Brown RD III *et al.* Permeability of liposomal membranes to water: results from the magnetic field dependence of T1 of solvent protons in suspensions of vesicles with entrapped paramagnetic ions. *Magn. Reson. Med.* 23(2), 275–286 (1992).

36 Kabalka GW, Davis MA, Buonocore E, Hubner K, Holmberg E, Huang L. Gadolinium-labeled liposomes containing amphipathic agents for magnetic resonance imaging. *Invest. Radiol.* 25(Suppl. 1), S63–S64 (1990).

37 Kabalka GW, Buonocore E, Hubner K, Davis M, Huang L. Gadolinium-labeled liposomes containing paramagnetic amphipathic agents: targeted MRI contrast agents for the liver. *Magn. Reson. Med.* 8(1), 89–95 (1988).

38 Kim SK, Pohost GM, Elgavish GA. Fatty-acyl iminopolycarboxylates: lipophilic bifunctional contrast agents for NMR imaging. *Magn. Reson. Med.* 22(1), 57–67 (1991).

39 Marcucci F, Lefoulon F. Active targeting with particulate drug carriers in tumor therapy: fundamentals and recent progress. *Drug Discov. Today* 9(5), 219–228 (2004).

40 Torchilin VP. Antibody-modified liposomes for cancer chemotherapy. *Expert Opin. Drug Deliv.* 5(9), 1003–1025 (2008).

41 Sofou S, Sgouros G. Antibody-targeted liposomes in cancer therapy and imaging. *Expert Opin. Drug Deliv.* 5(2), 189–204 (2008).

▪ **Authors review recent advances in the field of the immuno-liposomes (antibody-mediated targeting) with an emphasis on preclinical studies and place them in the context of historical developments.**

42 Wu H, Chang DK. Peptide-mediated liposomal drug delivery system targeting tumor blood vessels in anticancer therapy. *J. Oncol.* DOI: 10.1155/2010/723798 (2010). (Epub ahead of print).

▪▪ **Reviews the mechanisms and advantages of various present and potential methods using peptide-conjugated liposomes to specifically destroy tumor blood vessels in anticancer therapy.**

43 Torchilin VP. Recent advances with liposomes as pharmaceutical carriers. *Nat. Rev. Drug Discov.* 4(2), 145–160 (2005).

44 Allen TM. Ligand-targeted therapeutics in anticancer therapy. *Nat. Rev. Cancer* 2, 750–763. (2002).

45 van Tilborg GAF, Mulder WJM, Deckers N *et al*. Annexin A5-functionalized bimodal lipid-based contrast agents for the detection of apoptosis. *Bioconjug. Chem.* 17(3), 741–749 (2006).

46 Mulder WJM, Strijkers GJ, van Tilborg GAF, Cormode DP, Fayad ZA, Nicolay K. nanoparticulate assemblies of amphiphiles and diagnostically active materials for multimodality imaging. *Acc. Chem. Res.* 42(7), 904–914 (2009).

▪▪ **Authors describe the use of multifunctional lipid-based nanoparticles containing a variety of imaging agents for visualizing macrophages in atherosclerotic plaques.**

47 Bull SR, Guler MO, Bras RE, Maede TJ, Stupp SI. Self-assembled peptide amphiphile nanofibers conjugated to MRI contrast agents. *Nano Lett.* 5(1), 1–4 (2005).

48 Mulder WJM, Strijkers GJ, Griffioen AW *et al.* A liposomal system for contrast-enhanced magnetic resonance imaging of molecular targets. *Bioconjug. Chem.* 15(4), 799–806 (2004).

49 Mulder WJM, Strijkers GJ, Briley-Saebo KC *et al*. Molecular imaging of macrophages in atherosclerotic plaques using bimodal PEG-micelles. *Magn. Reson. Med.* 58(6), 1164–1170 (2007).

50 Lipinski MJ, Amirbekian V, Frias JC *et al.* MRI to detect atherosclerosis with gadolinium-containing immunomicelles targeting the macrophage scavenger receptor. *Magn Reson. Med*. 56(3), 601–610 (2006).

51 Amirbekian V, Lipinski MJ, Briley-Saebo KC *et al*. Detecting and assessing macrophages *in vivo* to evaluate atherosclerosis noninvasively using molecular MRI. *Proc. Natl Acad. Sci. USA* 104(3), 961–966 (2007).

▪ **Targeted immunomicelles able to detect and assess macrophages in atherosclerotic plaque by MRI. *In vivo* MRI revealed that at 24 h post-injection, immuno-micelles provided a 79% increase in signal intensity of atherosclerotic aortas, compared with only 34% using untargeted micelles.**

52 Li KCP, Bednarski MD. Vascular-targeted molecular imaging using functionalized polymerized vesicles. *J. Magn. Res. Imaging* 16(4), 388–393 (2002).

53 Storrs RW, Tropper FD, Li HY *et al.* Paramagnetic polymerized liposomes: synthesis, characterization, and applications for magnetic resonance imaging. *J. Am. Chem. Soc.* 117(28), 7301–7306 (1995).

54 Sipkins DA, Cheresh DA, Kazemi MR, Nevin LM, Bednarski MD, Li KCP. Detection of tumor angiogenesis *in vivo* by αvβ3-targeted magnetic resonance imaging. *Nat. Med.* 4(5), 623–626 (1998).

55 Sipkins DA, Gijbels K, Tropper FD, Bednarski MD, Li KCP, Steinman L. ICAM-1 expression in autoimmune encephalitis visualized using magnetic resonance imaging. *J. Neuroimmunol.* 104(1), 1–9 (2000).

56 Bull SR, Guler MO, Bras RE, Venkatasubramanian PN, Stupp SI, Maede TJ. Magnetic resonance imaging of self-assembled biomaterial scaffolds. *Bioconjug. Chem.* 16(6), 1343–1348 (2005).

57 Mulder WJM, Strijkers GJ, Habets JW *et al.* MR molecular imaging and fluorescence microscopy for identification of activated tumor endothelium using a bimodal lipidic nanoparticle. *FASEB J.* 19(14), 2008–2010 (2005).

58 Mulder WJM, van der Schaft DWJ, Hautvast PAI *et al.* Early *in vivo* assessment of angiostatic therapy efficacy by molecular MRI. *FASEB J.* 21(2), 378–383 (2007).

59 Brandwijk RJ, Mulder WJ, Nicolay K, Mayo KH, Thijssen VL, Griffioen AW. Anginex-conjugated liposomes for targeting of angiogenic endothelial cells. *Bioconjug. Chem.* 18(3), 785–790 (2007).

60 Kluza E, van der Schaft DW, Hautvast PA *et al.* Synergistic targeting of αvβ3 integrin and galectin-1 with heteromultivalent paramagnetic liposomes for combined MR imaging and treatment of angiogenesis. *Nano Lett.* 10(1), 52–58 (2010).

▪▪ ***In vitro* targeting efficacy of nanoparticles functionalized with two angiogenesis-specific targeting ligands, an $\alpha_v\beta_3$ integrin-specific and a galectin-1-specific peptide by optical and MRI techniques. The dual-targeting approach produces synergistic targeting effects, causing a dramatically elevated uptake of nanoparticles as compared with single-ligand targeting.**

61 Ferrari M. Cancer nanotechnology: opportunities and challenges. *Nat. Rev. Cancer* 5(3), 161–171 (2005).

▪▪ **Nanotechnology is a multidisciplinary field, which includes nanovectors for the targeted delivery of anticancer drugs and imaging contrast agents. Nanowires and other nanodevices can provide essential breakthroughs in the fight against cancer.**

62 Vaccaro M, Mangiapia G, Radulescu A *et al.* Colloidal particles composed of amphiphilic molecules binding gadolinium complexes and peptides as tumor-specific contrast agents in MRI: physico–chemical characterization. *Soft Matter* 5(13), 2504–2512 (2009).

63 Accardo A, Tesauro D, Roscigno P *et al.* Physicochemical properties of mixed micellar aggregates containing CCK peptides and Gd complexes designed as tumor specific contrast agents in MRI *J. Am. Chem. Soc.* 126, 3097–3107 (2004).

▪▪ **First example of mixed micelle containing CCK8 bioactive peptide able to drive a large amount of paramagnetic gadolinium ions to tumor tissue as a new potential contrast agent in MRI technique.**

64 Mangiapia G, Accardo A, Lo Celso F *et al.* Mixed micelles composed of peptides and gadolinium complexes as tumor-specific contrast agents in MRI: a SANS study. *J. Phys. Chem. B* 108, 17611–17617 (2004).

65 Vaccaro M, Accardo A, Tesauro D *et al.* Supramolecular aggregates of amphiphilic gadolinium complexes as blood pool MRI/MRA contrast agents: physicochemical characterization. *Langmuir* 22(15), 6635–6643 (2006).

66 Accardo A, Tesauro D, Morelli G *et al.* High-relaxivity supramolecular aggregates containing peptide and Gd complex agents in MRI. *J. Biol. Inorg. Chem.* 12, 267–276 (2007).

67 Tesauro D, Accardo A, Gianolio E *et al.* Peptide derivatized lamellar aggregates as target-specific MRI contrast agents. *ChemBioChem* 8, 950–955 (2007).

68 Vaccaro M, Accardo A, D'Errico G et al. Peptides and Gd complexes containing colloidal assemblies as tumor specific contrast agents in MRI: physicochemical characterization. *Biophys. J.* 93, 1736–1746 (2007).

69 Vaccaro M, Mangiapia G, Paduano L *et al.* Structural and relaxometric characterization of peptide aggregates containing gadolinium complexes as potential selective contrast agents in MRI. *ChemPhysChem* 8, 2526–2538 (2007).

▪ **Supramolecular aggregates based on a monomer with an upsilon shape (*MonY*) that contains, in the same molecule, the hydrophobic moiety that allows the formation of supramolecular aggregates, the bioactive CCK8 peptide for target recognition, and the gadolinium complex.**

70 Accardo A, Tesauro D, Aloj L *et al.* Peptide containing aggregates as selective nanocarriers for therapeutics. *ChemMedChem* 3, 594–602 (2008).

▪ ***In vitro* and *in vivo* studies on selective nanocarriers loaded with anticancer drug. Nanoparticles show desired specific targeting to cholecistokynin receptors, long plasma half-life, high stability and no acute side effects after intravenous injection in nude mice.**

71 Accardo A, Tesauro D, Del Pozzo L, Mangiapia G, Paduano L, Morelli G. Micelles by self-assembling peptide-conjugate amphiphile: synthesis and structural characterization. *J. Pept. Sci.* 14, 903–910 (2008).

72 Vaccaro M, Mangiapia G, Accardo A *et al.* Polymerized mixed aggregates containing gadolinium complex and CCK8 peptide. *Colloid Polym. Sci.* 286, 1643–1652 (2008).

73 Accardo A, Tesauro D, Morisco A *et al.* Micelles obtained by aggregation of gemini surfactants containing the CCK8 peptide and a gadolinium complex. *J. Biol. Inorg. Chem.* 14, 587–599 (2009).

▪ **Authors present supramolecular aggregates based on gemini surfactants with high relaxivity and target selectivity as potential contrast agents in MRI.**

74 Morisco A, Accardo A, Tesauro D, Palumbo R, Benedetti E, Morelli G. Peptide labeled supramolecular aggregates as selective doxorubicin carriers for delivery to tumor cells. *Biopolymers* DOI: 10.1002/bip.21491 (2010)(Epub ahead of print).

75 Accardo A, Mansi R, Morisco A *et al.* Peptide modified nanocarriers for selective targeting of bombesin receptors. *Mol. Biosyst.* 6, 878–887 (2010).

▪▪ **Reports the first example of liposomes derivatized by bombesin peptides able to target gastrin-releasing peptide receptors overexpressed in several human tumors. *In vitro* and *in vivo* experiments on PC-3 cells confirm their ability to specifically target and concentrate in receptor-expressing xenografts.**

76 Morisco A, Accardo A, Gianolio E, Tesauro D, Benedetti E, Morelli G. Micelles derivatized with octreotide as potential target selective contrast agents in MRI. *J. Pept. Sci.* 15, 242–250 (2009).

77 Accardo A, Morisco A, Gianolio E *et al.* octreotide as target-selective delivery tool of nanoparticles for MRI application. *J. Pept. Sci.* DOI: 10.1002/psc.1308 (2010) (Epub ahead of print).

78 Silvente-Poirot S, Dufresne M, Vaysse N, Fourmy D. The peripheral cholecystokinin receptors. *Eur. J. Biochem.* 215, 513–529 (1993).

79 Wank SA. Cholecystokinin receptors. *Am. J. Physiol.* 269, G628–G646 (1995).

80 Reubi JC, Schaer JC, Waser B. Cholecystokinin (CCK)-A and CCK-B/gastrin receptors in human tumors. *Cancer Res.* 57(7), 1377–1386 (1997).

81 Dufresne M, Seva C, Fourmy D. Cholecystokinin and gastrin receptors. *Physiol. Rev.* 86(3), 805–847 (2006).

82 Pellegrini M, Mierke DF. Molecular complex of cholecystokinin-8 and *N*-terminus of the cholecystokinin A receptor by NMR spectroscopy. *Biochemistry* 38, 14775–14783 (1999).

83 Aloj L, Caraco C, Panico M *et al. In vitro* and *in vivo* evaluation of $^{111}$In-DTPAGlu-G-CCK8 for cholecystokinin-B receptor imaging. *J. Nucl. Med.* 45(3), 485–494 (2004).

84 Battey JF, Way JM, Corjay MH *et al.* Molecular cloning of the bombesin/gastrin-releasing peptide receptor from Swiss 3T3 cells. *Proc. Natl Acad. Sci. USA* 88(2), 395–399 (1991).

85 Fathi Z, Corjay MH, Shapira H *et al.* BRS-3: a novel bombesin receptor subtype selectively expressed in testis and lung carcinoma cells. *J. Biol. Chem.* 268(8), 5979–5984 (1993).

86 Nagalla SR, Barry BJ, Creswick KC, Eden P, Taylor JT. Cloning of a receptor for amphibian [Phe-13]bombesin distinct from the receptor for gastrin-releasing peptide: identification of a fourth bombesin receptor subtype (BB4). *Proc. Natl Acad. Sci. USA* 92(13), 6205–6209 (1995).

87 Wada E, Way J, Shapira H. cDNA cloning, characterization, and brain region-specific expression of a neuromedin-B-preferring bombesin receptor. *Neuron* 6(3), 421–430 (1991).

88 Markwalder R, Reubi JC. Gastrin-releasing peptide receptors in the human prostate: relation to neoplastic transformation. *Cancer Res.* 59(5), 1152–1159 (1999).

89 Gugger M, Reubi JC. Gastrin-releasing peptide receptors in non-neoplastic and neoplastic human breast. *Am. J. Pathol.* 155(6), 2067–2076 (1999).

90 Fleischmann A, Waser B, Reubi JC. Overexpression of gastrin-releasing peptide receptors in tumor-associated blood vessels of human ovarian neoplasms. *Cell Oncol.* 29(5), 421–433 (2007).

91 Smith CJ, Volkert WA, Hoffman TJ. Radiolabeled peptide conjugates for targeting of the bombesin receptor superfamily subtypes. *Nucl. Med. Biol.* 32(7), 733–740 (2005).

92 Lamberts SWJ. Somatostatin analogues from one decade to the second. In: *octreotide: the Next Decade.* Lamberts SWJ (Ed.). Bristol Bioscientifica, UK 3–65 (1999).

93 Bauer W, Briner U, Doepfner W. SMS 201–995: a very potent and selective octapeptide analogue of somatostatin with prolonged action. *Life Sci.* 31, 1133–1140 (1982).

94 Veber DF, Freidinger RM, Schwenk-Perlow D *et al.* A potent cyclic hexapeptide analogue of somatostatin. *Nature* 292, 55–58 (1981).

95 Kowalski J, Henze M, Schuhmacher J, Mäcke HR, Hofmann M, Haberkorn U. Evaluation of positron emission tomography imaging using [$^{68}$Ga]-DOTA-D-Phe-(1)-Tyr-(3)-octreotide in comparison to [$^{111}$In]-DTPAOC SPECT. First results in patients with neuroendocrine tumors. *Mol. Imaging Biol.* 5, 42–48 (2003).

96 Reubi JC, Waser B, Schaer JC, Laissue JA. Somatostatin receptor sst1-sst5 expression in normal and neoplastic human tissues using receptor autoradiography with subtype-selective ligands. *Eur. J. Nucl. Med.* 28, 836–846; Erratum in: *Eur. J. Nucl. Med.* 28, 1433 (2001).

97 Bell G, Reisine T. Molecular biology of somatostatin receptors. *Trends Neurosci.* 16, 34–38 (1993).

98 Reubi JC, Horisberger U, Laissue J. High density of somatostatin receptors in veins surrounding human cancer tissue: role in tumor host interaction? *Int. J. Cancer* 56, 681–688 (1994).

99 Reubi JC, Schaer JC, Waser B, Mengod G. Expression and localization of somatostatin receptor SSTR1, SSTR2, and SSTR3 messenger RNAs in primary human tumors using *in situ* hybridization. *Cancer Res.* 54, 3455–3459 (1994).

100 Reubi JC. Peptide receptors as molecular targets for cancer diagnosis and therapy. *Endocr. Rev.* 24(4), 389–427 (2003).

101 Anelli PL, Lattuada L, Lorusso V, Schneider M, Tournier H, Uggeri F. Mixed micelles containing lipophilic gadolinium complexes as MRA contrast agents. *MAGMA* 12(2–3), 114–120 (2001).

102 Accardo A, Tesauro D, Mangiapia G, Pedone C, Morelli G. Nanostructures by self-assembling peptide amphiphile as potential selective drug carriers. *Biopolymers* 88, 115–121 (2007).

103 Delli Castelli D, Gianolio E, Geninatti Crich S, Terreno E, Aime S. Metal containing nanosized systems for MR-molecular imaging applications. *Coord. Chem. Rev.* 252(21–22), 2424–2443 (2008).

104 Accardo A, Tesauro D, Aloj L, Pedone C, Morelli G. Supramolecular aggregates containing lipophilic Gd(III) complexes as contrast agents in MRI. *Coord. Chem. Rev.* 253(17–18), 2193–2213 (2009).

▪▪ **Reports on the state-of-the-art of supramolecular aggregates of lipophilic gadolinium complexes, correlating their structural and relaxometric properties. Aggregates derivatized with peptides and antibodies acting as target-selective MRI contrast agents are described.**

105 Menger FM, Littau CA. Gemini-surfactants: synthesis and properties. *J. Am. Chem. Soc.* 113, 1451–1452 (1991).

106 Zana R. Dimeric and oligomeric surfactants. Behavior at interfaces and in aqueous solution: a review. *Adv Colloid Interface Sci.* 97(1–3), 205–253 (2002).